CO_2 hydrogenation in a dielectric barrier discharge plasma revealed

CO_2 Hydrogenation in a Dielectric Barrier Discharge Plasma Revealed

Christophe De Bie,[†] *Jan van Dijk*[‡] *and Annemie Bogaerts**[,†]

[†] Research Group PLASMANT, Department of Chemistry, University of Antwerp, Universiteitsplein 1, 2610 Wilrijk-Antwerpen, Belgium

[‡] Department of Applied Physics, Eindhoven University of Technology, Den Dolech 2, Postbus 513, 5600 MB Eindhoven, The Netherlands

* E-mail: annemie.bogaerts@uantwerpen.be Telephone: +32 (0)3 265 2377.

Abstract: The hydrogenation of carbon dioxide in a dielectric barrier discharge plasma is studied with a one-dimensional fluid model. The spatially averaged densities of the most important end products formed in the CO_2/H_2 mixture are determined as a function of the initial gas mixing ratio. CO and H_2O are found to be present at the highest densities and to a lower content also CH_4, C_2H_6, CH_2O, CH_3OH, O_2, and some other higher hydrocarbons and oxygenates. The main underlying reaction pathways for the conversion of the inlet gases and the formation of CO, CH_4, CH_2O, and CH_3OH are pointed out for various gas mixing ratios. The CO_2 conversion and the production of value added products is found to be quite low, also in comparison to a CO_2/CH_4 mixture, and this can be explained by the model.

1. Introduction

Global warming, due to CO_2 emissions, is one of the major problems of the 21st century. CO_2 is a very stable molecule that requires a lot of energy to be activated for the majority of synthetic routes to produce chemicals. Therefore, a first objective in the mitigation of CO_2 emissions is the process of carbon dioxide capture and storage (CCS), as pointed out in a special report published in 2005 by the Intergovernmental Panel on Climate Change.[1] Nowadays, it is clear that aside from the reduction of CO_2 emissions to the atmosphere and the use of CCS for this purpose, also the energy efficient utilization of (captured) CO_2, as an important carbon resource to create products, will be a crucial step in order to achieve an economically viable low-carbon economy.

Today, CO_2 utilization is mainly limited to the direct use, i.e., without a conversion step, as an inert agent for food packaging, in carbonated drinks, in refrigeration systems, in fire extinguishers, as a solvent, and for enhanced oil recovery (particularly in the United States), as well as the indirect use for the chemical production of mainly urea, a lower content of methanol and an even smaller amount of a wide variety of other products.[1-3] Ongoing research on the conversion of CO_2 in value added chemicals is primarily focusing on the formation of carbon monoxide (CO), methanol, polymers, urea, carboxylates, carbonates, olefins, etc.[2] In order to convert CO_2 into products, an energy source, such as heat or electricity, or material inputs, such as fly ash, hydrogen, or epoxides, is required.[2] To become of added value, it is crucial that new CO_2 utilization processes have a lower carbon footprint than their equivalent classical processes using fossil fuel routes for the production of the same product.

In the last decades, there is an increasing interest in using plasma technology for the conversion of gases such as CO_2. Several types of plasma reactors are being investigated for this purpose.[4] One example of such a plasma is the dielectric barrier discharge (DBD)[5-10] which can

be operated at atmospheric pressure and room temperature, and thus, it enables gas phase reactions at ambient conditions. A DBD is generated between two electrodes of which at least one is covered with a dielectric material. The gap between both electrodes is typically a few millimeters. An ac voltage with an amplitude of 1 - 100 kV and a frequency ranging from a few Hz to MHz is usually applied to this kind of discharges.

Current research on the use of plasma for CO_2 conversion includes the splitting of pure CO_2 into CO and O_2[11-35] and the direct synthesis of higher hydrocarbons, syngas, and oxygenates through the reforming of CH_4 by CO_2[36-94] or the hydrogenation of CO_2[95-98]. However, application of the latter is up to now limited because of the high cost of hydrogen.[39] The sustainable and economically viable production and use of H_2 will be of major importance to develop a competitive process for the hydrogenation of CO_2. Even more, an environmentally beneficial conversion process can only be realized if this process converts more CO_2 than the amount of CO_2 produced in the whole process including the H_2 manufacturing. Nowadays, H_2 is produced by steam reforming of CH_4, coal gasification, and partial oxidation of light oil residues. As a result, fossil fuels are depleted and the net atmospheric CO_2 emissions are increased.[99] Therefore, a lot of research is carried out concerning new H_2 production methods based on the use of renewable energy sources. Besides, also technologies for the production of H_2 from H_2O such as electrolysis, thermolysis, thermochemical splitting, photoelectrolysis, and photobiological cleavage are of interest.[100]

Recently, the interest in the development of new sustainable industrial processes for the direct hydrogenation of CO_2 into CH_3OH is increasing because of the potential of CH_3OH in a growing hydrogen economy. Methanol is a primary liquid petrochemical which is of great importance in the chemical and energy industries, because it can be easily stored and transported.[99] A direct

route to produce methanol would be more efficient and environmentally sustainable as it becomes more and more possible to make hydrogen gas in an economically efficient manner using renewable energy. Moreover, this hydrogenation process is a well-known reaction in catalysis research. Olah et al.[100] discussed the present understanding of the mechanism of the catalytic methanol synthesis from syngas. They concluded that CH_3OH is probably almost exclusively formed by hydrogenation of CO_2 contained in syngas on the catalytic surface. The CO in the syngas first undergoes a water-gas shift reaction to form CO_2 and H_2. The formed CO_2 then reacts with H_2 to yield CH_3OH. Furthermore, in view of the goal to reduce the atmospheric concentration of CO_2 and therefore decreasing our dependence on fossil fuels, the use of natural gas and his principal component CH_4 as a coreactant is of less interest. Therefore, if H_2 can be produced from H_2O by renewable energy sources, it is more interesting as H-source for CO_2 conversion than CH_4.

In order to develop an economically viable industrial process for the hydrogenation of CO_2 by means of a dielectric barrier discharge, it is crucial to first obtain a better insight into the complicated underlying plasma chemistry acting in the conversion process. Besides experimental work, computer modeling can offer here the necessary information.

Experimental and modeling investigations on the plasma chemistry in CO_2/H_2 mixtures reported in literature are, however, very rare. Eliasson et al.[95] investigated the hydrogenation of CO_2 to CH_3OH in a DBD with and without the presence of a catalyst. Experimentally the effects of combining a catalyst with a discharge on the yield of CH_3OH were analyzed for different reaction parameters, such as the gas temperature, the pressure, the inlet gas mixing ratio, the electric power, and the flow rate of the feed gas. Furthermore, a simplified semiempirical kinetic model was used to simulate the accumulated chemical action of many microdischarges, in order

to calculate the CH_3OH yield in the CO_2/H_2 discharge. A radical reaction mechanism was proposed for the formation of CH_3OH. Liu et al.[101] discussed in a review paper the use of nonthermal plasmas for CO_2 utilization, including the hydrogenation of CO_2 to form CH_3OH in a DBD, referring thereby to the work of Eliasson et al.[95] Hayashi et al.[96] discussed the decomposition of CO_2 in the presence of H_2 or water vapor by a nonthermal plasma, produced by a surface discharge at atmospheric pressure. CO, CH_4, dimethyl ether (C_2H_6O), formic acid (HCOOH), and water vapor were detected as end products of a gas mixture of 50% CO_2 and 50% H_2. Kano et al.[97] studied the reforming of CO_2 by H_2 to CH_4 and CH_3OH by using a radio frequency impulse low-pressure discharge under different discharge parameters. CH_4, CO, CH_3OH, and water vapor were found as end products. Recently Zeng et al.[98] investigated the plasma-catalytic CO_2 hydrogenation in a coaxial packed-bed DBD at low temperatures and atmospheric pressure. The performance of different γ-Al_2O_3 supported metal catalysts on the conversion of CO_2 was studied. The reverse water-gas shift reaction, i.e., the formation of CO and H_2O, as well as carbon dioxide methanation, i.e., the formation of CH_4 and H_2O, have been reported as the dominant reaction processes. The results also show that the H_2/CO_2 molar ratio significantly affects the conversion of CO_2 and the yields of CO and CH_4. Furthermore, some recent theoretical studies on the hydrogenation of CO_2 are worth mentioning, although they are not directly related to plasma chemistry. Chiavassa et al.[102] modeled the synthesis of CH_3OH from CO_2/H_2 on a Ga_2O_3-Pd/silica catalyst and Tao et al.[103] performed a density functional theory (DFT) study to investigate the reaction mechanisms for the synthesis of CH_3OH from CO_2 and H_2.

In the present paper, we present a 1D fluid modeling study for the conversion of CO_2, in the presence of H_2, into CO, higher hydrocarbons and higher oxygenates. The extensive chemistry

set used in this model was earlier developed and previously used to describe the plasma chemistry in an atmospheric pressure DBD in CH_4/O_2 and CH_4/CO_2 gas mixtures.[87] The formation of a variety of higher hydrocarbons and higher oxygenates in CO_2/H_2 for different gas mixing ratios is calculated, as well as the conversion of the inlet gases. These results will be compared with the experimental observations from the papers mentioned above on CO_2/H_2 gas discharges, as well as with earlier calculated results with the same model for a CH_4/CO_2 gas mixture. This will allow us to determine the best gas mixture, in terms of conversion and production of the various value-added end products considered in the model. Furthermore, the focus of the present paper is on the main underlying pathways governing the conversion of CO_2 with H_2, into the main reaction products, i.e., CO, CH_4, CH_2O, and CH_3OH, in order to explain the product formation in the different gas mixing ratios and to reveal why some oxygenates are formed while others seem not to be formed.

2. Description of the Model

A one-dimensional fluid model, called Plasimo's MD2D,[104-105] is applied. This fluid model consists of a set of coupled partial differential equations which are derived from the Boltzmann equation. More specifically, particle continuity equations and drift-diffusion equations for the various species, as well as an electron energy balance equation, are solved. These equations are coupled to the Poisson equation for a self-consistent calculation of the electric field. This set of coupled equations is solved in time and in space until periodic steady state is reached. A more detailed description of the physics used in the model and of the numerical methods that are applied, is reported by Hagelaar[106] and by Brok et al.[107] Detailed information about the specific use of the model for describing a detailed plasma chemistry in a DBD and the applied boundary conditions can be found in De Bie et al.[108]

The chemistry set developed for the CO_2/H_2 gas mixture is almost identical to the one constructed for a CH_4/O_2 and CH_4/CO_2 gas mixture, except for some adaptations of the third body species in the neutral-neutral three-body collision reactions, where CO_2 and H_2 are now included as third body instead of CH_4, O_2, CO_2, and H_2O, with the same rate coefficients. In total, 75 species (electrons, molecules, ions, and radicals) are included in the model, as presented in Table 1. Note that dimethyl ether (CH_3OCH_3) and formic acid (HCOOH), which were experimentally found by Hayashi et al.,[96] as mentioned above, are not included in the model as the rate constants for the formation and loss processes for these molecules are unknown. As a consequence, our model will not be able to make predictions on the formation of these products. We expect that these species would anyway play a minor role in the chemistry, especially as intermediates. They might be potential end products, but we do not expect their densities to be higher than, e.g., CH_4, CH_3OH, and CH_2O, and certainly much lower than, e.g., CO. In the future, however, we would like to take these species into account in our model as well, if data would become available to describe their chemistry. The 75 species included in the model interact with each other in 963 gas phase reactions, including 157 electron-neutral, 48 electron-ion, 420 neutral-neutral and 338 ion-ion or ion-neutral reactions. Detailed information on the construction of the chemistry set and the transport coefficients and wall interaction coefficients used in the model can be found in our earlier papers.[87, 108]

Table 1. Overview of the Species Included in the Model, besides the Electrons

molecules	CH_4, C_2H_6, C_2H_4, C_2H_2, C_2, C_3H_8, C_3H_6, C_4H_2, H_2, O_3, O_2, CO_2, CO, H_2O, H_2O_2, CH_2O, CH_3OH, C_2H_5OH, CH_3CHO, CH_2CO, CH_3OOH, C_2H_5OOH
ions	CH_5^+, CH_4^+, CH_3^+, CH_2^+, CH^+, C^+, $C_2H_6^+$, $C_2H_5^+$, $C_2H_4^+$, $C_2H_3^+$, $C_2H_2^+$, C_2H^+, C_2^+, H_3^+, H_2^+, H^+, O_4^+, O_2^+, O^+, O_4^-, O_3^-, O_2^-, O^-, CO_2^+, CO^+, H_3O^+, H_2O^+, OH^+, H^-, OH^-
radicals	CH_3, CH_2, CH, C, C_2H_5, C_2H_3, C_2H, C_3H_7, C_3H_5, H, O, OH, HO_2, CHO, CH_2OH, CH_3O, C_2H_5O, C_2HO, CH_3CO, CH_2CHO, CH_3O_2, $C_2H_5O_2$

The model is applied to a cylindrical atmospheric pressure DBD reactor setup, as described in our earlier work.[87, 108] The reactor consists of two coaxial electrodes of which the inner electrode is grounded and has an outer diameter of 22 mm. The outer electrode has a diameter of 29.3 mm and is powered by a high-voltage supply. It is wrapped around a dielectric material made of alumina. The alumina tube has an inner diameter of 26 mm and a wall thickness of 1.6 mm, resulting in a discharge gap of 2 mm. The length of the outer electrode, which defines the discharge length, is 120 mm. However, we only consider the radial direction, i.e., the direction between both electrodes, in the model, in order to limit the calculation time and especially to avoid that we have to deal with filament formation in the DBD reactor. Indeed, a DBD operating in a CO_2/H_2 mixture is not spatially homogeneous, but consists of a large number of microdischarge filaments which occur randomly in time, as well as in space along the axial direction.[33] This filament formation can, however, not be simulated with the present model. For this reason, we apply the model only in the radial direction, so that we do not have to deal with the spatial inhomogeneity (filaments) in the axial direction.

We assume that the gas temperature is 300 K, constant in time and in space. This is justified, because in a DBD there is only local heating due to the discharge filaments. However, the latter only take a very small fraction of the reactor volume for several nanoseconds, with a repetition in the microseconds scale, yielding a so-called volume-corrected filament frequency of about 0.02% per half discharge period.[109] This volume-corrected filament frequency was estimated in Bogaerts et al.[109] from experimental data of Ozkan et al.[33] on the filament lifetime and the number of filaments per half discharge cycle. More specifically, in these experiments, an average filament lifetime of 15.6 ns was measured, and about 200 filaments per half cycle were counted. Assuming a typical filament diameter of 0.1 mm in a gap size of 2 mm corresponds to a filament

volume of 0.016 mm^3.[109] The plasma reactor volume of Ozkan et al.[33] was 15.08 cm^3; hence, this yields a filament volume fraction of 1.04 x 10^{-6}. When we combine this with the measured number of filaments per half cycle (i.e., 200), this gives a so-called "volume-corrected filament frequency" of 2.08 x 10^{-4} (or 0.02%) per half cycle. Thus, as the filaments occupy only a small fraction of the discharge, both in space and in time, overall, the gas heating is very limited. Furthermore, often a water jacket is used in experiments to cool the reactor and keep the reactor temperature constant.[18, 36, 110-113] More information about the reactor setup can be found in our previous papers.[87, 108]

The calculations are carried out as a function of time, up to 20s. This time corresponds to the gas residence time in the reactor. Thus, the gas conversion and product yields for shorter residence times (corresponding to higher gas flow rates) will also follow automatically from these model calculations. Furthermore, a sinusoidal voltage with amplitude of 5 kV and frequency of 10 kHz is applied. The CO_2 fraction in the CO_2/H_2 mixture is varied from 10 to 90%.

3. Results and Discussion

First, the spatially averaged electron density and temperature, and radical densities as a function of time and initial gas mixing ratio will be illustrated. Subsequently, the densities of the formed end products, as well as their yields and selectivities and the conversion of the inlet gases as a function of the initial gas mixing ratio will be presented. Finally, the dominant reaction pathways for the conversion of the inlet gases and the formation of CO, CH_4, CH_2O and CH_3OH will be pointed out for the various gas mixing ratios. A comparison will be made with our

previous work on the conversion in a CO_2/CH_4 gas mixture, to determine which gas mixture would be more suitable for producing specific value added products.

3.1. Densities of the Plasma Species

The plasma chemistry in a DBD is initiated by the electrons, which are heated by the electric field and give rise to electron impact excitation, ionization, and dissociation collisions. The excited species, ions and radicals created in this way, will then further react into the formation of new molecules. The spatially averaged electron density and temperature, as well as the densities of the radicals and ions produced in the plasma, exhibit periodic behavior as a function of time, following the period of the applied sinusoidal voltage. Periodic steady state is reached after 0.001 s. Figure 1 shows the spatially averaged electron density and temperature as a function of time, for four periods of the applied voltage, for a 50/50 CO_2/H_2 gas mixture. It is clear that the electron density varies from peak values of 10^{18} m^{-3} in the beginning of each period to virtually zero in the rest of the period, while the spatially averaged mean electron energy varies between 0.7 and 3.8 eV. The overall spatially and time averaged electron density for all CO_2/H_2 gas mixtures under study amounts to ca. 10^{15} m^{-3}, while the overall spatially and time averaged mean electron energy varies between 1.9 and 2.7 eV. These results are similar to the values calculated in pure CH_4[108] and in the CH_4/O_2 and CH_4/CO_2 gas mixtures[87]. Also the ion densities show a similar periodic behavior, as was illustrated in our earlier work.[87, 108]

Note that an electron density of ca. 10^{15} m^{-3} is a typical value for the filaments in a DBD,[4, 114] where the electron impact collisions are initiated, while a mean electron energy between 1.9 and 2.7 eV also is typical inside the filaments[4, 114]. This indicates that our model, neglecting the filaments, will still give a realistic estimate of the plasma chemistry.

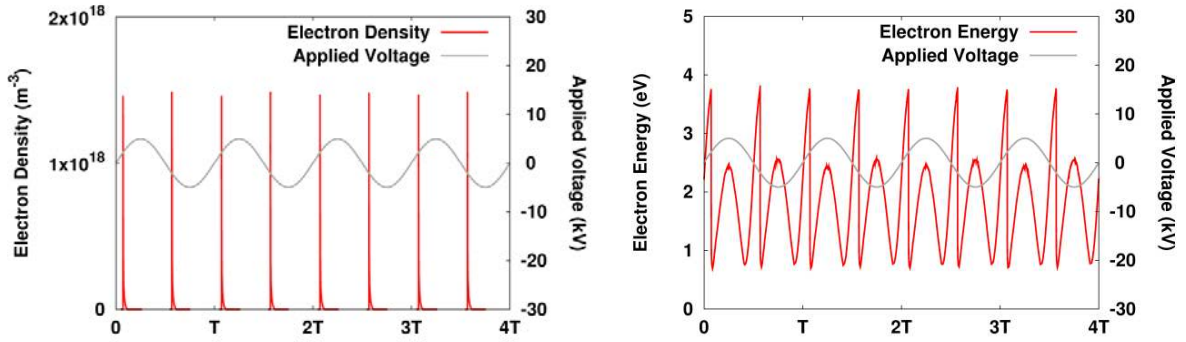

Figure 1. Spatially averaged electron density (a) and energy (b) as a function of time for a 50/50 CO_2/H_2 gas mixture, on a linear scale, as well as the applied sinusoidal voltage (gray, right axis) for four periods of the applied voltage (i.e., between 0.0016 and 0.002 s).

Figure 2 illustrates the periodic behavior of the most important radical densities for a 50/50 CO_2/H_2 gas mixture, for four periods of the applied voltage. Only the CH_3 and CH_2 radicals vary over a wide range as a function of time within one period of the applied voltage, while the other radicals show only a minor (~ 10%) periodic variation (H, O, OH), or almost no periodic variation at all (HO_2, CHO). The periodic trend is here superimposed on a rising trend, acting over a longer time scale until periodic steady state is reached. The H atoms are the most abundant radicals, with an overall spatially and time averaged density of about 10^{20} m^{-3}, followed by the O atoms, OH, HO_2, and CHO radicals, which have densities in the order of 10^{19}, 10^{17}, 10^{15}, and 10^{15} m^{-3}, respectively. The CH_3 and CH_2 radicals only have spatially and time averaged densities in the order of 10^{11} m^{-3}. The reason why most of these radicals, except CH_2, do not vary a lot as a function of time within one period is because the formation of all these radicals proceeds in a quite similar way, i.e., either directly or indirectly related to electron impact dissociation of the inlet gases. However, CH_2 is rapidly destructed in reactions with CO_2, one of the inlet gases, which is thus present at high density, explaining the significant drop in the CH_2

density as a function of time, while H, O, OH, HO_2, CHO, and CH_3 react away through collisions with other radicals or molecules at lower densities. The most abundant radicals will determine the different reaction pathways for the formation of different end products (see below). Compared to our previous results for the CO_2/CH_4 mixture[87], the higher order hydrocarbon radicals, such as C_2H_5 and C_2H_3, as well as the oxygenate radicals, such as CH_3O, CH_2OH, and CH_3O_2, are formed to a lower extent in CO_2/H_2, which is logical, as there is no hydrocarbon precursor (CH_4) in the inlet gas mixture, resulting in a lower overall carbon fraction than in CO_2/CH_4.

The spatially and time averaged densities of the most abundant radicals in CO_2/H_2 are plotted in Figure 3 as a function of the initial CO_2 in the mixture. Upon rising the initial fraction of CO_2 between 10 and 90 %, the densities of the H, CH_3, and CH_2 radicals drop by 1 order of magnitude, because these radicals are directly or indirectly formed out of H_2. On the other hand, the densities of O, OH, HO_2, and CHO, as well as the other O-containing radicals (not shown), increase by one order to several orders of magnitude upon rising the inlet fraction of CO_2, as they are directly or indirectly formed out of CO_2.

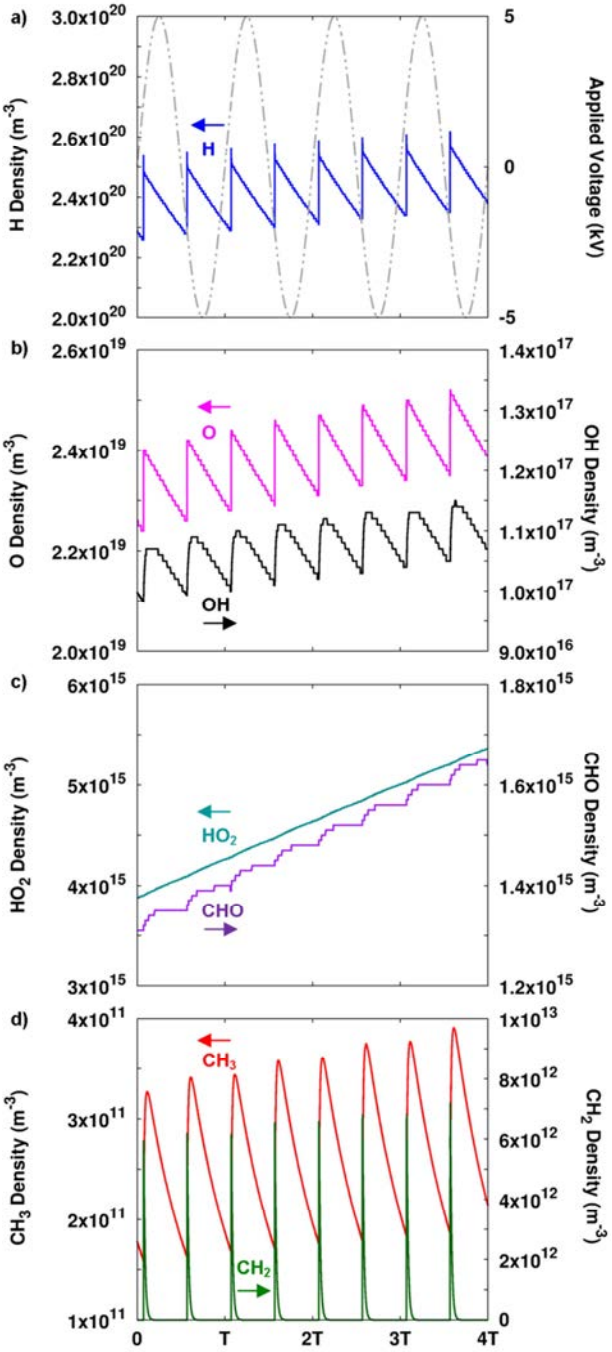

Figure 2. Spatially averaged radical densities as a function of time for a 50/50 CO_2/H_2 gas mixture, as well as the applied sinusoidal voltage (gray, right axis in (a)) for four periods of the applied voltage (i.e., between 0.0016 and 0.002 s).

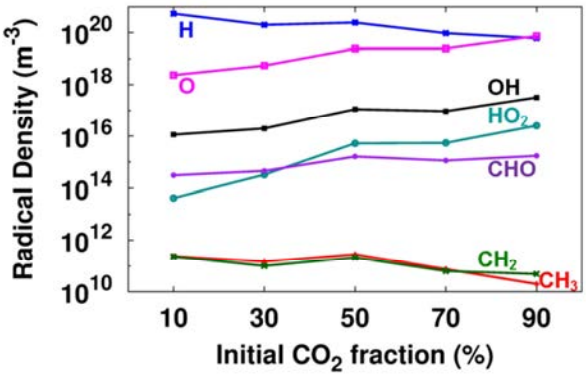

Figure 3. Spatially and time averaged (taken over 1 period, i.e., between 0.0019 and 0.002 s) radical densities as a function of the initial CO_2 fraction in the CO_2/H_2 gas mixture.

The most abundant ion in the CO_2/H_2 gas mixture is H_3O^+, with a spatially and time averaged density in the order of 10^{15} m^{-3}, hence comparable to the electron density (cf. above). The other ion densities are 2 or even more orders of magnitude lower, and thus the ion densities are much lower than the spatially and time averaged densities of the most abundant radicals, indicating that the ions play a minor role in the plasma chemistry (see also sections 3.3 and 3.4 below). Therefore, we do not go in further detail on the ion densities.

The densities of the stable molecules do not exhibit a periodic behavior like the electrons and the radicals. The reason is that their formation rates are typically much larger than their loss rates, in contrast to the radials and ions. The densities of the molecules formed during the hydrogenation of CO_2, i.e., CO, higher order hydrocarbons and oxygenates, exhibit a rising trend as a function of time, because their net production is higher than their net consumption. This will continue until periodic steady state will be reached. Indeed, when the densities of the reaction products rise, the rates of their consumption reactions will rise as well, until a balance is reached between production and consumption. The inlet gases, on the other hand, have a higher net

consumption, so their densities show a gradual decrease as a function of time again until periodic steady state will be reached. The initial densities of the inlet gases, at a 50/50 gas mixture, both amount to 1.22 x 10^{25} m^{-3}, as calculated from the ideal gas law at 300 K and 1 atm. The conversion is most pronounced in the first few seconds, and afterward the densities of the molecules do not significantly change anymore for a longer residence time, as is clear from Figure 4, for both CO_2 and H_2, and the most abundant products.

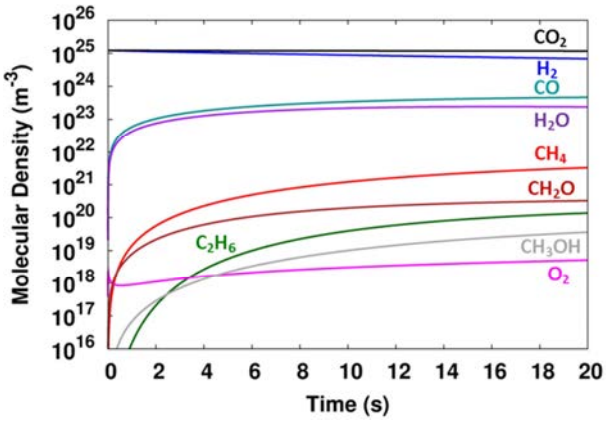

Figure 4. Spatially averaged molecular densities as a function of the residence time for a 50/50 CO_2/H_2 gas mixture.

Figure 5 illustrates the densities of the various molecules in the CO_2/H_2 gas mixture as a function of the initial CO_2 fraction, after a residence time of 5 s. The most abundant reaction products are CO, H_2O, CH_4, CH_2O, C_2H_6, O_2, and CH_3OH (more or less in order of decreasing density). This is in good agreement with the end products reported by Eliasson et al.[95], i.e., CH_4 and CH_3OH, Hayashi et al.[96], i.e., CO and CH_4, Kano et al.[97], i.e. CO, CH_4 and CH_3OH, and Zeng et al.[98], i.e. CO and H_2O as major products, a small amount of CH_4 and traces of C_2H_6, for similar CO_2/H_2 discharges. Note that Hayashi et al.[96] also detected the formation of dimethyl ether and formic acid, which are not included in our model as mentioned above. However, our

model provides us more insight in the formation of other higher hydrocarbons and oxygenates. The densities of CO and H_2O, which are by far the most abundant products, are almost not influenced by the inlet fraction of CO_2 (see Figure 5a). For H_2O, a maximum is obtained at an initial CO_2 fraction of 50%. This can be explained because H_2O is formed out of the collision of OH and H radicals. From Figure 3 it is clear that the H density decreases while the OH density increases with increasing initial CO_2 fraction, resulting in an optimum ratio at an inlet concentration of 50% CO_2. Furthermore, as will be clear from section 3.2 below, the CO_2 conversion drops upon increasing initial CO_2 fraction in the mixture, and thus, the same applies to the yield of CO. On the other hand, a higher initial CO_2 fraction in the mixture allows for more CO_2 to be converted, and as both effects compensate each other, the effective CO_2 conversion remains constant, explaining why the CO density is constant for all CO_2/H_2 gas mixtures (see Figure 5a).

On the other hand, the densities of O_2, H_2O_2, and O_3 increase by several orders of magnitude upon increasing initial fraction of CO_2, which is logical, as they are directly formed out of the CO_2 splitting products (O and O_2). The densities of the higher hydrocarbons (C_xH_y) generally drop upon increasing initial fraction of CO_2, which can be explained by the higher conversion of CO_2 at lower initial fraction of CO_2 (see section 3.2 below) resulting in higher densities of CH_2 and CH_3 radicals, as is clear from Figure 3 above, which are the building blocks for the higher hydrocarbons. However, an optimum seems to be reached for the 50/50 CO_2/H_2 gas mixture (see Figure 5b). Indeed, these higher hydrocarbons need the C from CO_2 as their building block, but they also need the H originating from H_2, and therefore an equal presence of both inlet gases seems to be preferable.

The same is true for the densities of CH_2O and CH_3OH and the other oxygenates, as is clear from Figure 5(c), although the hydroperoxides (CH_3OOH and C_2H_5OOH) generally increase with rising initial fraction of CO_2. Compared to our previous results on the formation of higher hydrocarbons and oxygenates in CH_4/O_2 and CH_4/CO_2 mixtures[87], it is clear that, except for CO and H_2O, the densities of the most important end products are now several orders of magnitude lower. The reason for this is that the conversion of CO_2 is very low in all gas mixtures (see section 3.2 below), while CH_4 as C building block was more easily converted[87], and therefore, the crucial radicals in the formation process of higher hydrocarbons and oxygenates, such as CH_2 and CH_3, can be produced at a much higher density in mixtures with CH_4 than in the CO_2/H_2 mixture under study here. Note that the trends illustrated in Figure 5 correspond to a residence time of 5 s; however, the different molecules might have their maximum densities at a different residence time for the different gas mixing ratios studied (see for instance De Bie et al.[87] for the CH_4/O_2 and CH_4/CO_2 mixtures); therefore, the trends depicted in Figure 5 are not necessarily the same at other residence times.

Altering the inlet gas mixing ratio also affects the H_2/CO (syngas) ratio. A variable H_2/CO molar ratio is useful, as it allows the mixture to be used for various industrial synthesis processes, while classical processes, like steam reforming, partial oxidation, and dry reforming typically produce syngas with a H_2/CO molar ratio greater than 3, less than 2, and less than 1, respectively. [37, 45] The H_2/CO ratio, as obtained from our calculations, decreases with increasing initial CO_2 fraction, which is logical. It ranges from 54 (at 10% CO_2), which is not useful for industrial synthesis processes, to 3 (at 90% CO_2), which can be of interest as this is similar to the molar ratio produced by steam reforming (see above).

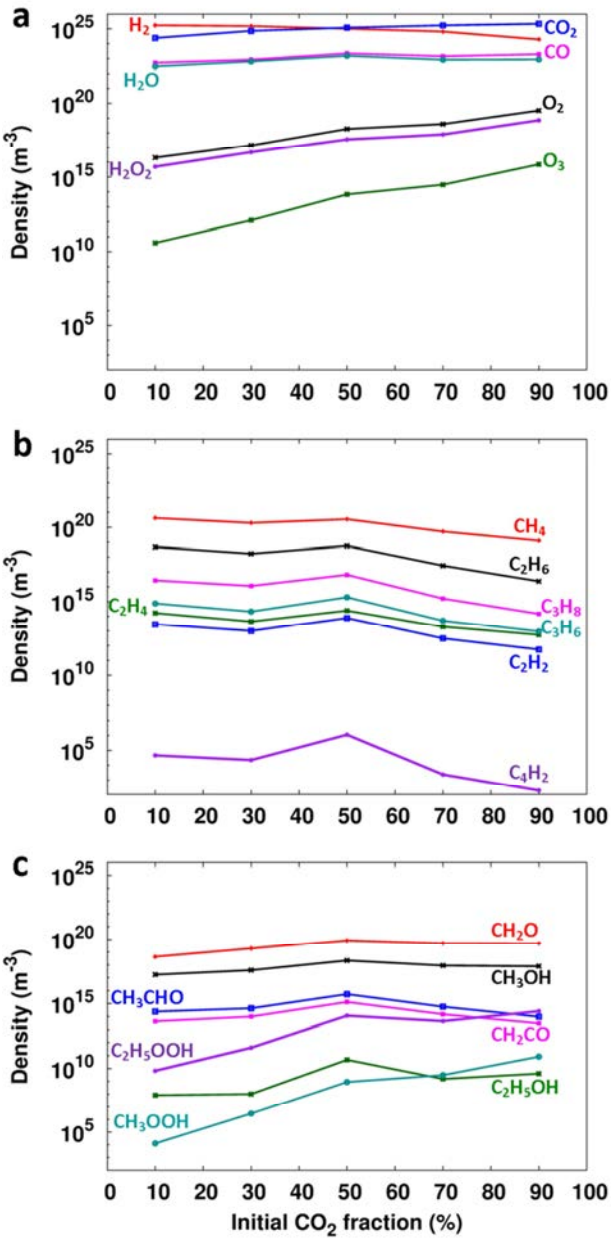

Figure 5. Spatially averaged molecule densities as a function of the initial CO_2 fraction in the CO_2/H_2 gas mixture, after a residence time of 5 s.

3.2. Conversion of CO_2 and H_2 and Yields and Selectivities of the Main Reaction Products

The following definitions are used for calculating the conversion X of the inlet gases, and the yields Y and the selectivities S of most interesting end products, such as CO, the higher hydrocarbons and higher oxygenates:

$$X_{CO_2/H_2} = \frac{n_{CO_2/H_2,converted}}{n_{CO_2/H_2,feed}} \times 100\ \% \qquad (1)$$

$$Y_{C_xH_yO_z} = \frac{x \times n_{C_xH_yO_z}}{n_{CO_2,feed}} \times 100\ \% \qquad (2)$$

$$S_{C_xH_yO_z} = \frac{x \times n_{C_xH_yO_z}}{n_{CO_2,converted}} \times 100\ \% \qquad (3)$$

The parameter x in these definitions denotes the stoichiometric balance coefficient, which corresponds also to the index in the compound name of $C_xH_yO_z$. Note that the yield and selectivity of CO are calculated with $Y_{C_xH_yO_z}$ and $S_{C_xH_yO_z}$, respectively, with y = 0, and that the yield and selectivity of the higher hydrocarbons (C_xH_y) are calculated with $Y_{C_xH_yO_z}$ and $S_{C_xH_yO_z}$, respectively, with z = 0.

Table 2 shows the maximum conversions of the inlet gases, i.e. CO_2 and H_2, and the maximum yields and corresponding selectivities of CO and CH_4, for different CO_2/H_2 gas mixtures. These maximum values are in all cases obtained for a residence time of 20 s. The conversion of CO_2 clearly decreases with increasing initial CO_2 fraction in the mixture, from 7% at 10% CO_2 in the mixture to roughly 2% at 90% CO_2 in the mixture. This trend is in good agreement with the results of Zeng et al.[98], who reported that the conversion of CO_2 increases almost linearly with the increase of the H_2/CO_2 molar ratio at a fixed flow rate. A similar trend was earlier observed in CO_2/CH_4, but the conversion of CO_2 was a factor of 3 higher at a high initial CH_4 fraction

(i.e., 90%) compared to a high initial H_2 fraction of 90%. This can be explained because CH_2, which is a direct dissociation product of CH_4, is much more abundant in CO_2/CH_4 than in CO_2/H_2 and thus provides an extra and very important loss process for CO_2 in a CO_2/CH_4 mixture.[87] The H_2 conversion is significantly larger, i.e., between 30 and 60 %, but no clear trend can be observed as a function of gas mixing ratio, because the discharge characteristics are strongly affected by the initial gas mixing ratio. As CO is directly produced by electron impact dissociation of CO_2 (see section 3.3 below), the yield of CO shows the same trend as the conversion of CO_2, with values of only 2-6 %. Moreover, CO is the only C containing molecule directly produced out of CO_2, and therefore the selectivity of CO is in all cases around 90%. CH_4 is only formed with a selectivity above 1% at a low initial CO_2 fraction, i.e., a high initial H_2 fraction, which is logical. The yields of C_2H_6, CH_2O, and CH_3OH are one or 2 orders of magnitude lower than the yield of CH_4, while the yields of other higher hydrocarbons and oxygenates are even more negligible, which is of course the direct result of the rather low conversion of CO_2 in all gas mixing ratios. Note that also some sticking of the C atoms and hydrocarbon species at the walls occurs, which explains why the sum of the selectivities is not equal to 100 %. This formation of a C-containing layer on the electrodes was indeed also experimentally observed in the DBD reactor under study for a pure CO_2 discharge.[30, 115]

Table 2. Overview of the Maximum Conversions of the Inlet Gases, i.e., CO_2 and H_2, and the Maximum Yields and Corresponding Selectivities of CO and CH_4 for Different CO_2/H_2 Gas Mixtures.

initial CO_2 fraction	X (CO_2)	X (H_2)	Y (CO) - S (CO)	Y (CH_4) - S (CH_4)
10	7.0	64	6 - 86	0.2 - 2.2
30	3.6	33	3 - 90	0.03 - 0.9
50	4.4	44	4 - 87	0.03 - 0.6
70	2.1	33	2 - 89	0.003 - 0.2
90	1.9	58	2 - 92	0.0003 - 0.02

[a] All values are noted as percentages.

3.3. Dominant Reaction Pathways

To better explain the above trends, and to find out how the densities of the most important products can be optimized, it is crucial to obtain a better insight in the underlying reaction chemistry. Therefore, we will now discuss the dominant reaction pathways for the conversion of the inlet gases into the most important value-added products, i.e., CO, CH_4, CH_3OH, and CH_2O, for the entire range of gas mixing ratios.

3.3.1. Dissociation of CO_2 and H_2

The dominant reactions for CO_2 consumption (and production), as well as the time-averaged total production rate, total loss rate and net loss rate, as a function of the initial CO_2 fraction in the gas mixture are depicted in Figure 6. Although the consumption of CO_2 is mostly relevant in this work, we also show the production processes, because part of the CO_2 dissociation products will again recombine into the formation of CO_2. However, the total loss rate is larger than the total production rate, as is clear from Figure 6, thus leading to a net loss of CO_2 (i.e., conversion into other products). Furthermore, the total formation and loss rate generally increase upon larger

initial CO_2 fraction in the mixture, which is logical. The most important channel for consumption of CO_2 is electron impact ionization toward CO_2^+. However, CO_2^+ immediately reacts back toward CO_2 upon charge transfer with H_2O molecules. Therefore, the most important reaction for consumption of CO_2 is effectively electron impact dissociation toward CO. This result was also obtained in earlier simulations carried out in our group for pure CO_2 splitting.[27] Furthermore, the relative importance of the various consumption and production processes is more or less independent from the gas mixing ratio, as is clear from Figure 6.

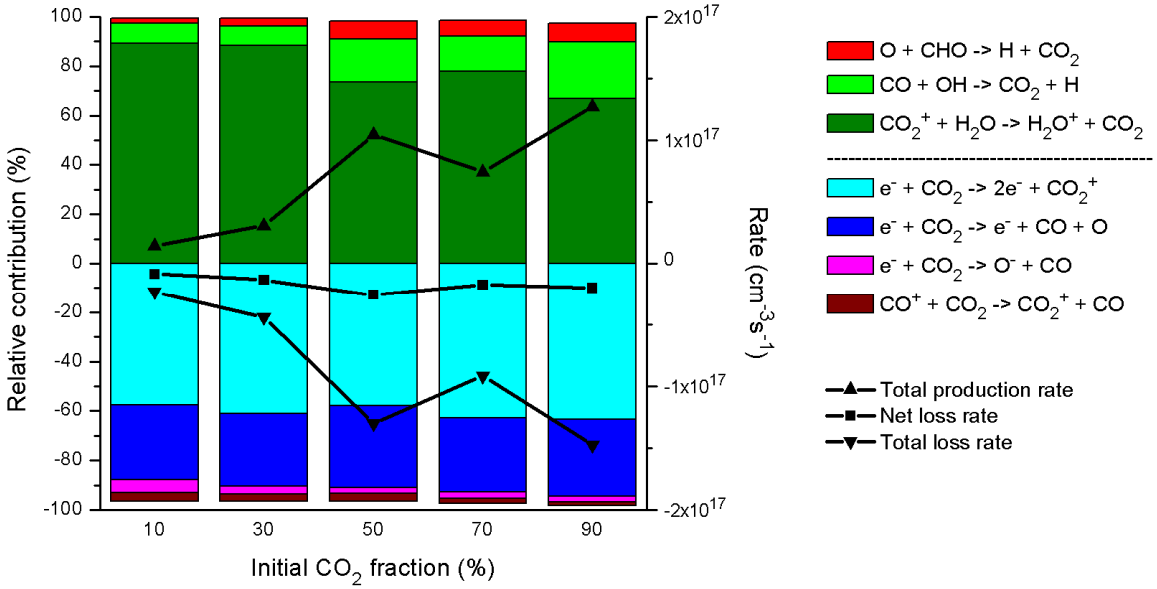

Figure 6. Relative contributions of the various production and consumption processes of CO_2 (left axis), as well as the time-averaged total production rate, total loss rate, and net loss rate (right axis), as a function of the initial CO_2 fraction in the CO_2/H_2 gas mixture. The production rates are defined as positive values, while the consumption rates are plotted as negative values. The time-averaged values are taken over the entire simulation time (i.e., 0 – 20 s). This also applies to the following figures.

In Figure 7 the most important reactions for consumption (and production) of H_2 are shown. At an initial CO_2 inlet fraction of 10%, electron impact dissociation is the most important loss process for H_2, but part of the H atoms will recombine back into H_2, or react with CHO radicals into H_2 and CO. At an inlet fraction of 90% CO_2 the reaction of H_2 with H_2O^+ toward H_3O^+ becomes the most important loss mechanism. However, the latter is not due to the high absolute rate of this reaction but rather because the rate of electron impact dissociation drops. Indeed, it is clear from Figure 7 that the total loss rate of H_2 is much lower at 90% than at 10% CO_2 content, because there is of course less H_2 in the mixture. Nevertheless, from comparing Figures 6 and 7, it is clear that the net consumption of H_2 is much higher than the net consumption of CO_2. Indeed, the net loss rate of H_2 drops from 7 x 10^{17} cm^{-3} s^{-1} at 10% CO_2 to 7 x 10^{16} cm^{-3} s^{-1} at 90% CO_2, while the net loss rate of CO_2 is virtually constant around 10^{16} cm^{-3} s^{-1} for all gas mixing ratios. This explains also why the conversion of H_2 is much higher than the conversion of CO_2 (see section 3.2 above).

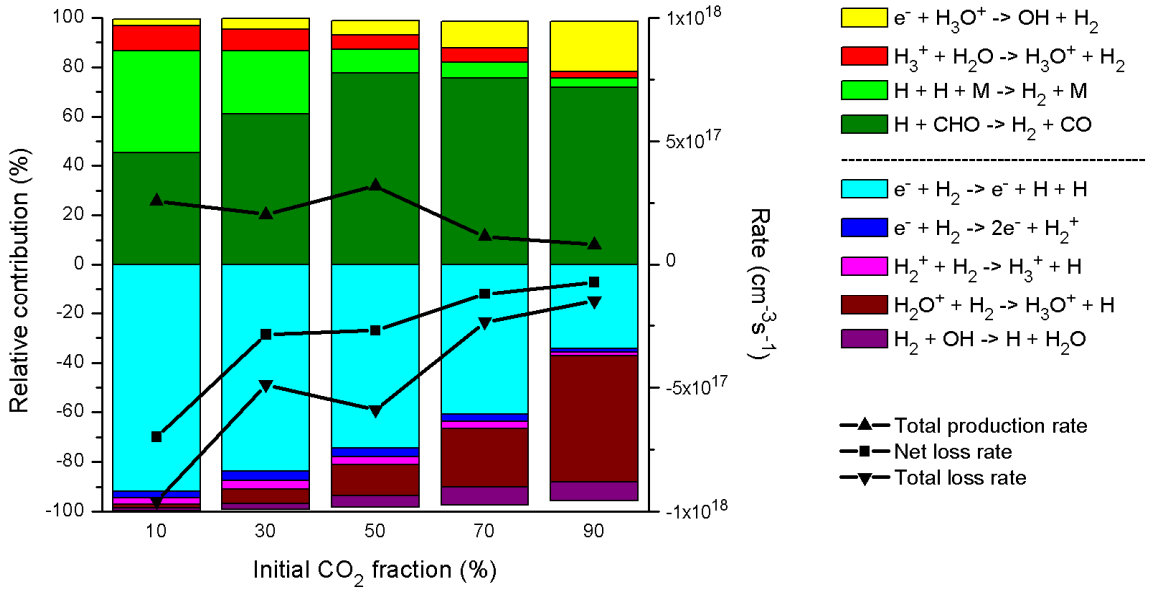

Figure 7. Relative contributions of the production and consumption processes of H_2 (left axis), as well as the time-averaged total production rate, total loss rate, and net loss rate (right axis), as a function of the initial CO_2 fraction in the CO_2/H_2 gas mixture.

3.3.2. Formation of CO, CH_4, CH_2O, and CH_3OH

In Figure 8 the most important channels for the production (and loss) of CO are illustrated as a function of the initial CO_2 fraction in the gas mixture. The most important production process appears to be the reaction between H atoms and CHO radicals, forming H_2 and CO, but this reaction is counterbalanced by the most important loss process, i.e., the recombination of H with CO into CHO radicals. Therefore, the most important effective reaction for the formation of CO is electron impact dissociation of CO_2. On average there is a net formation of CO, with a rate in the order of 10^{16} $cm^{-3}s^{-1}$, slightly increasing upon higher initial CO_2 fraction in the mixture, which is logical.

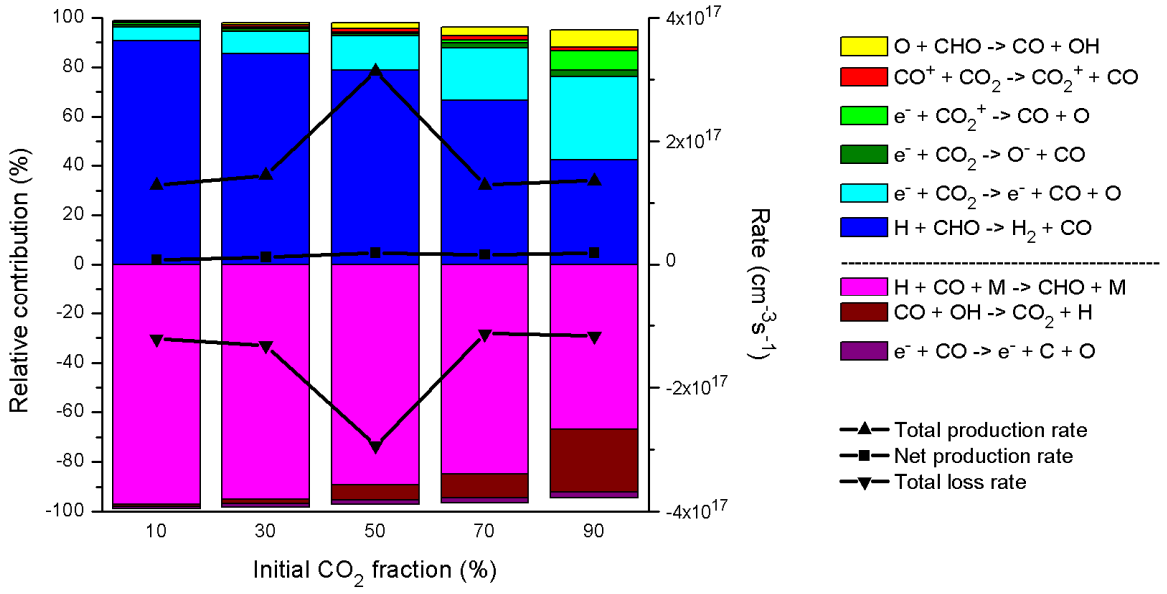

Figure 8. Relative contributions of the production and consumption processes of CO (left axis), as well as the time-averaged total production rate, total loss rate, and net production rate (right axis), as a function of the initial CO_2 fraction in the CO_2/H_2 gas mixture.

The most important reactions for production (and loss) of CH_4 are depicted in Figure 9 as a function of the initial CO_2 fraction in the gas mixture. The production of CH_4 seems to be driven by only two reactions, i.e., the three-body recombination reaction between CH_3 and H radicals, and at a lower initial fraction of CO_2 also the charge transfer reaction between CH_5^+ and H_2O. However, the latter reaction is partially balanced by the loss of CH_4 via a charge transfer reaction with H_3^+. At a higher initial CO_2 fraction, the charge transfer reaction with CO_2^+ becomes the most important loss mechanism for CH_4. A similar trend is observed for the net production rate of CH_4 as a function of the initial CO_2 fraction as for the net loss rate of H_2 (see Figure 7 above). Indeed, the dissociation of H_2 leads to the formation of H radicals which are needed for the

formation of CH_4. An optimum is obtained for an initial CO_2 fraction of 10%, as is logical, and can be explained by the maximum densities found for the CH_3 and H radicals, as shown in Figure 3 above.

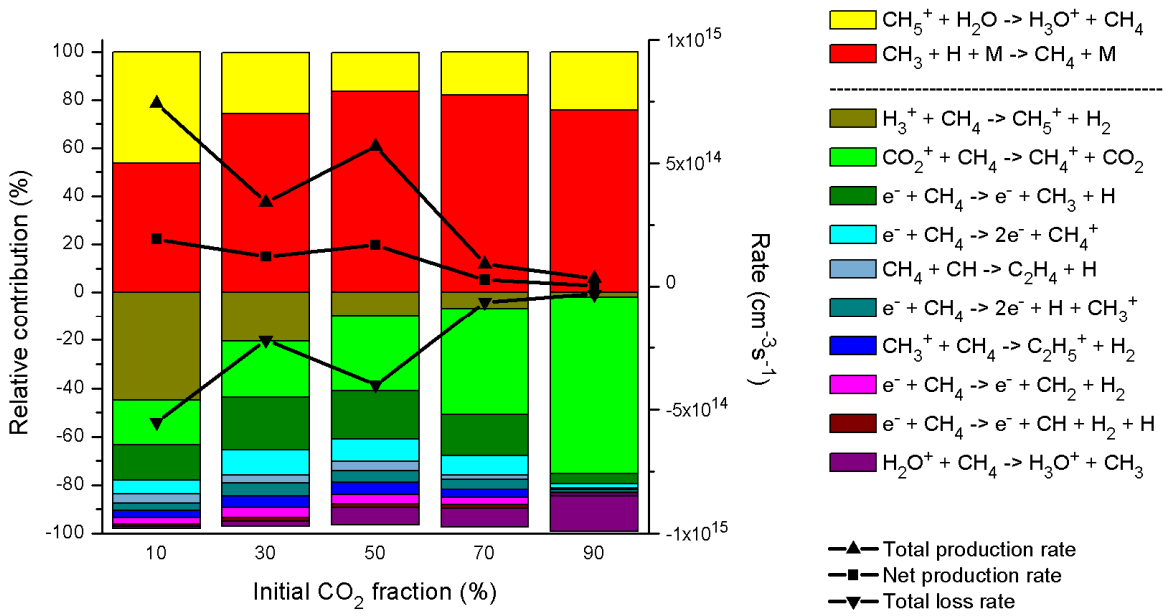

Figure 9. Relative contributions of the production and consumption processes of CH_4 (left axis), as well as the time-averaged total production rate, total loss rate, and net production rate (right axis), as a function of the initial CO_2 fraction in the CO_2/H_2 gas mixture.

Figures 10 and 11 show the dominant reactions for production (and loss) of CH_2O and CH_3OH, respectively, as a function of the initial CO_2 fraction in the gas mixture. The reaction between CO_2 and CH_2 radicals appears to be the most important channel for the production of formaldehyde at low initial CO_2 fractions, as was also observed for a CO_2/CH_4 mixture[87]. At higher initial CO_2 fractions, CH_2O is also formed to some extent out of two CHO radicals.

Furthermore, CH_2O is mainly lost upon collision with H atoms, yielding CHO and H_2, although the collisions with O atoms or OH radicals, yielding CHO and OH or H_2O, respectively, become gradually more important at higher CO_2 fractions, which is logical.

The total formation and loss rates reach a clear maximum at 50% CO_2 in the mixture, which is explained by the fact that at these conditions an optimum ratio of CH_2 (see the maximum in Figure 3 above) and CO_2 is present in the gas mixture. As the total formation and loss rates are more or less equal to each other, the net formation rate of CH_2O is very low, and increases from 10^{11} to 10^{13} $cm^{-3}s^{-1}$ upon rising CO_2 fraction. This explains why the CH_2O density rises slightly upon increasing CO_2 fraction in the mixture, as illustrated in Figure 5 above.

As is clear from Figure 11, the most important channel for the production of methanol, as predicted by our model, is the three-body reaction between CH_3 and OH radicals, like was also the case in the CO_2/CH_4 mixture studied before[87]. However, different from the CO_2/CH_4 mixture, the three-body reaction between CH_2OH and H radicals is now also an important production channel. Most of the CH_3OH produced is also consumed again upon collision with either H atoms, OH radicals, or O atoms, so the net formation rate of CH_3OH varies from 10^{11} to 10^{12} $cm^{-3}s^{-1}$. An optimum production of CH_3OH is again observed at 50/50 CO_2/H_2, because at these conditions an optimum ratio of CH_3 and OH (see Figure 3 above) is present in the gas mixture, and this explains why the CH_3OH density reaches a maximum at this mixing ratio, as shown in Figure 5 above.

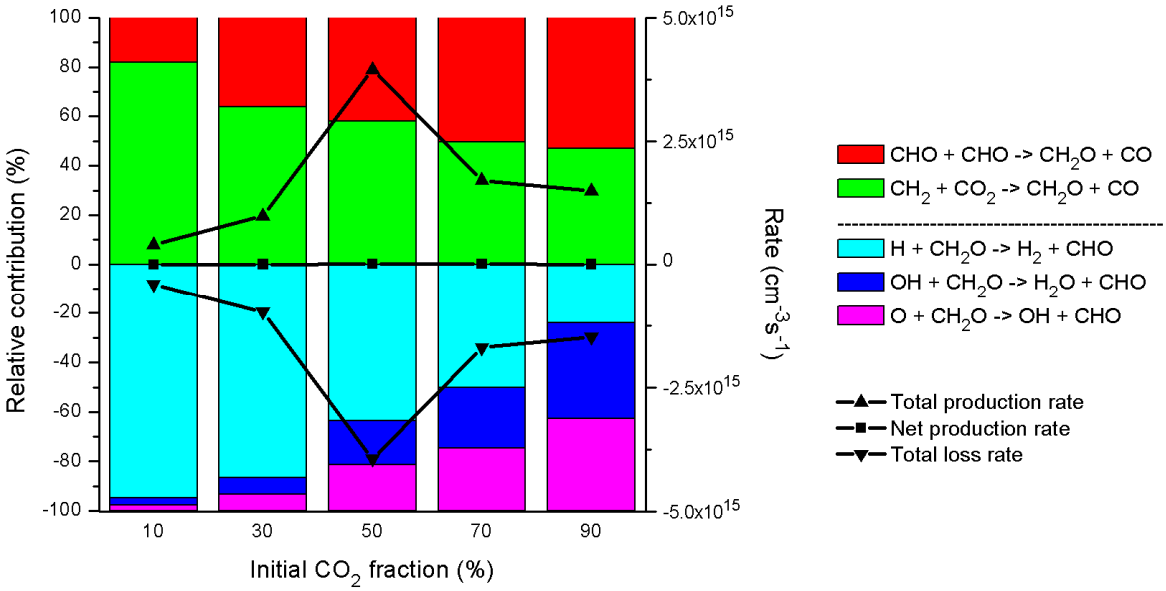

Figure 10. Relative contributions of the production and consumption processes of CH_2O (left axis), as well as the time-averaged total production rate, total loss rate, and net production rate (right axis), as a function of the initial CO_2 fraction in the CO_2/H_2 gas mixture.

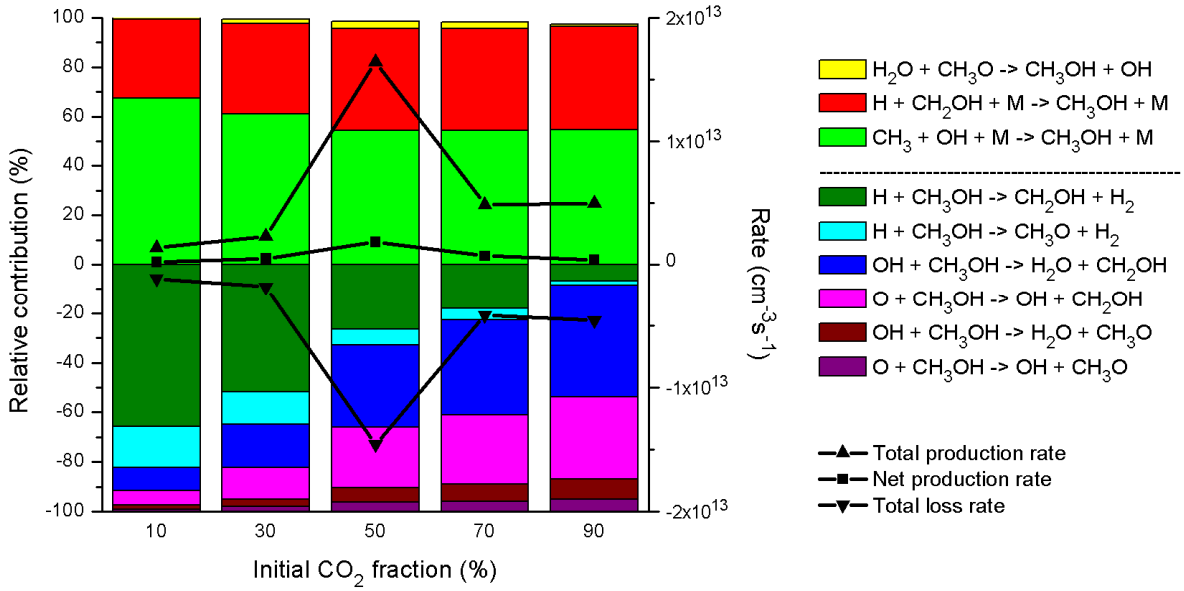

Figure 11. Relative contributions of the production and consumption processes of CH_3OH (left axis), as well as the time-averaged total production rate, total loss rate, and net production rate (right axis), as a function of the initial CO_2 fraction in the CO_2/H_2 gas mixture.

3.4. Overall Reaction Mechanism for the Hydrogenation of CO_2 into Valuable Products

Figure 12 summarizes the dominant reaction pathways for the conversion of CO_2 and H_2 in a 50/50 CO_2/H_2 gas mixture. Note that the thickness of the arrow lines is proportional to the rates of the net reactions. The conversion starts with electron impact dissociation of CO_2, yielding CO and O radicals. Simultaneously, and much more pronounced, is the electron impact dissociation of H_2, resulting in the formation of H radicals (cf. the thickness of the arrow line). Radical recombination reactions of the O and H radicals lead to the formation of OH radicals, which recombine further into H_2O, and this explains why H_2O is also formed at relatively high density,

as shown in Figure 5 above. However, this is of course of lesser interest than CO as valuable product.

CO will partially react back into CO_2, mainly through the formation of CHO radicals. Note that in this gas mixture, the major reaction from CO back into CO_2 indeed proceeds through CHO, as the rate of the reaction ($CO + H + M \rightarrow CHO + M$) is in the order of 10^{17} cm^{-3} s^{-1}, and the rate of the subsequent formation of CO_2 through the reaction ($CHO + O \rightarrow CO_2 + H$) is about 7×10^{15} cm^{-3} s^{-1}, while the rate of the direct reaction ($CO + O + M \rightarrow CO_2 + M$) is only in the order of 10^{15} cm^{-3} s^{-1}. The H atoms thus contribute significantly to the back reaction of CO into CO_2. It is clear from the thick arrow line from H to CHO in Figure 12 that the formation of CHO out of CO and H indeed occurs at a very high rate. The reason why the arrow line from CO to CHO is much thinner is because CHO also reacts back into CO upon collision with H ($CHO + H \rightarrow CO + H_2$), so the net reaction from CO to CHO is smaller than the net reaction from H to CHO. Furthermore, electron impact dissociation of CO results in the formation of C radicals, which react further into CH, CH_2, C_2HO and CH_3 radicals in several successive radical recombination reactions. The formed CH_2 radicals react with CO_2 into the formation of CH_2O, as was also shown in Figure 10 above. The CH_3 radicals easily form CH_4, which is much more favored (i.e., the rate is 1 order of magnitude larger) than the formation of CH_3OH out of CH_3. CH_4 partially reacts further into higher hydrocarbons (C_xH_y).

From the reaction scheme, it is clear that a lot of subsequent radical reactions are necessary for the formation of (higher) hydrocarbons and oxygenates, such as CH_4, C_2H_6, CH_2O, and CH_3OH, which explains the very low yields and selectivities of these end products (see section 3.2 above). Indeed, the lack of direct formation of CH_2 and CH_3 in CO_2/H_2, which is important in CO_2/CH_4 gas mixtures[87], combined with the very low conversion of CO_2, which is again due to

the absence of CH_2 as important collision partner for the loss of CO_2, makes a CO_2/H_2 mixture under the present conditions less interesting for the formation of higher hydrocarbons and oxygenates than a CO_2/CH_4 mixture. This is especially true because H_2 itself is a useful product, while CH_4, besides being a fuel itself, also greatly contributes to global warming, and thus, the simultaneous conversion of CO_2 and CH_4 will reduce the concentration of two greenhouse gases. Moreover, CO_2/CH_4 mixtures are available from biomass installations, and their simultaneous conversion can be seen as a direct valorization of biogas, instead of the energy intensive biogas upgrading to a CH_4-rich gas by removing CO_2. Another possibly interesting H-source to be added to a CO_2 plasma to produce value added chemicals, could be water, and the combined CO_2/H_2O conversion could even mimic the natural photosynthesis process. However, recent investigations in our group have illustrated that this gas mixture is also not able to produce oxygenates above the ppm range in a DBD plasma. Moreover, adding H_2O to a CO_2 plasma was found to even yield a drop in the CO_2 conversion, because the OH radicals formed out of H_2O splitting in the plasma, recombine with CO molecules back into CO_2. Moreover, as H_2O is electronegative, it will trap the electrons, making the discharge less stable, and there will also be less electrons available for CO_2 dissociation. Hence, all this indicates that a CO_2/H_2O DBD plasma (without catalysts) might also not be an optimal choice for CO_2 conversion into value-added chemicals.[4]

In general, we believe that a CO_2/H_2 mixture can be of interest for producing CO, to obtain gas mixtures with a specific H_2/CO ratio. However, besides the CO_2 conversion and CO yield, also the energy efficiency of the CO_2 conversion into CO is a key performance indicator for this technology. The energy efficiency is calculated from the CO_2 and H_2 conversion, the reaction enthalpy (ΔH_R), and the specific energy input (SEI), with the following formula:

$$\eta(\%) = \frac{\Delta H_R \left(\frac{kJ}{mol}\right) * X_{overall}(\%)}{SEI\left(\frac{kJ}{L}\right) * 24.6\left(\frac{L}{mol}\right)} \qquad (4)$$

The overall conversion is obtained by multiplying the absolute conversion of the inlet gases with their inlet fraction:

$$X_{overall}\ (\%) = X_{CO_2}(\%) * [CO_2]\ (\%) + X_{H_2}(\%) * [H_2](\%) \qquad (5)$$

The SEI is obtained from the plasma power, divided by the gas flow rate, as follows:

$$SEI\left(\frac{kJ}{L}\right) = \frac{\text{Plasma power (kW)}}{\text{Flow rate } \left(\frac{L}{min}\right)} * 60\left(\frac{s}{min}\right) \qquad (6)$$

As CO is the main product in our study, the reaction we consider for calculating the energy efficiency for the hydrogenation of CO_2 is as follows:

$$CO_2 + H_2 \rightarrow CO + H_2O \qquad (7)$$

$$\Delta H_R = 41.2\ \frac{kJ}{mol} = 0.427 \frac{eV}{molecule}\ \ (at\ 298\ K) \qquad (8)$$

Using these formulas, an energy efficiency of 0.92 % is obtained at a residence time of 2 s for a corresponding conversion of 1.1 % CO_2 and 8.0 % H_2 in 50/50 CO_2/H_2. Similar values are obtained for the other gas mixtures. These values are very low, indicating that a relatively high SEI of 8.3 kJ L^{-1} is required to obtain only a conversion of 1.1 % CO_2. Note that this energy efficiency is lower than the values obtained for pure CO_2 splitting or dry reforming of methane, which are typically in the order of 1-10 %.[27, 72, 77-78, 85, 91] However, also the latter values are still quite low, and indicate that a normal DBD reactor might not be competitive with classical thermal processes for CO_2 conversion. Indeed, the limited energy efficiency is a major drawback of a DBD plasma, as also reported in literature (e.g., Aerts et al.[27]). However, this value can be improved by inserting a dielectric packing in the DBD reactor. Indeed, the dielectric packing yields enhanced electric fields in the plasma, due to polarization of the dielectric beads, resulting in higher electron energies.[116] The latter gives rise to more electron impact excitation, ionization,

and dissociation of CO_2 for the same applied power and thus a higher energy efficiency. This is indeed illustrated in several papers, where simultaneous improvements in both the CO_2 conversion and energy efficiency of a factor 2 were reported.[24, 28, 117]

Furthermore, this so-called packed bed DBD reactor can also be combined with a catalyst packing (or catalytic coating on the dielectric packing), yielding so-called plasma catalysis.[118] This will enable the selective production of value-added chemicals, like specific oxygenated compounds. The latter was demonstrated by Eliasson et al.[95], who reported much higher methanol yields in the presence of a catalyst in the plasma, and by Zeng et al.[98], who found that the combination of a plasma with a catalyst enhances the conversion of CO_2 by 7-36 %, as well as the yield and energy efficient production of CO.

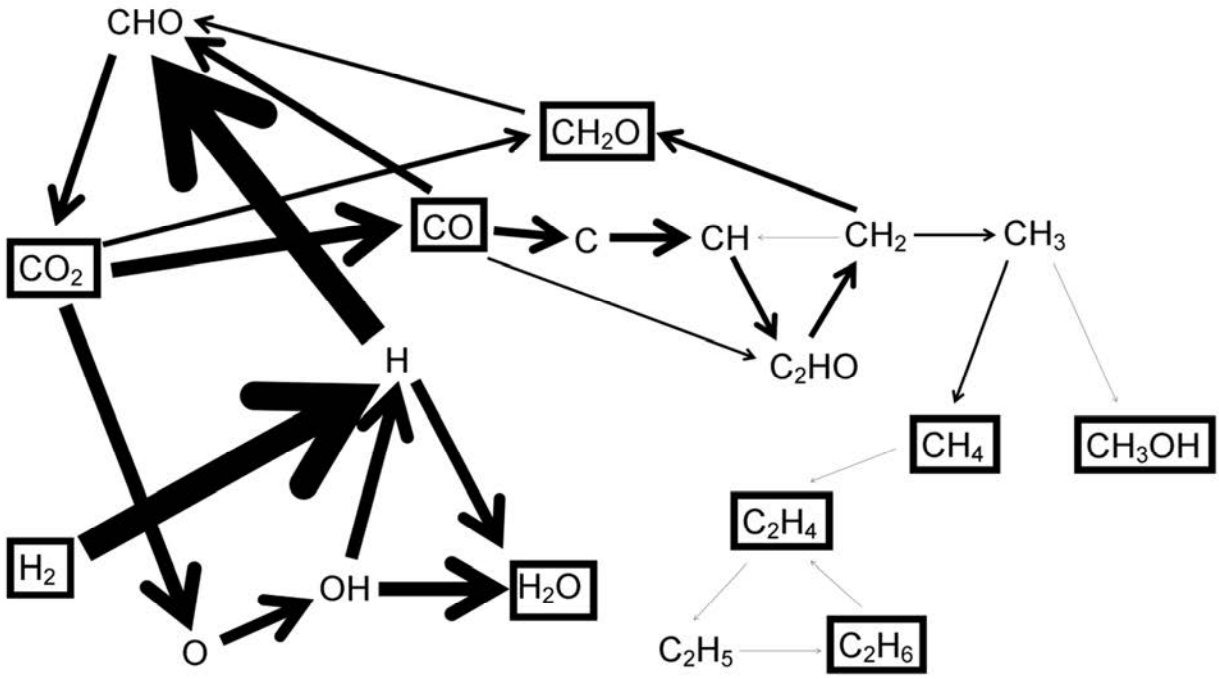

Figure 12. Dominant reaction pathways for the conversion of CO_2 and H_2 into various products, in a 50/50 CO_2/H_2 gas mixture. The thickness of the arrow lines is proportional to the rates of the net reactions. The stable molecules are indicated with black rectangles.

4. Conclusions

A 1D fluid modeling study for the hydrogenation of CO_2 in a DBD plasma was carried out for different CO_2/H_2 gas mixing ratios. The densities of the various plasma species as a function of the residence time and the gas mixing ratio were discussed. The spatially averaged densities of the electrons, radicals and ions produced in the plasma exhibit periodic behavior as a function of time, following the period of the sinusoidal applied voltage. The most abundant radicals are H, O, OH, HO_2, CHO, CH_3, and CH_2. The densities of the molecules formed during the hydrogenation of CO_2, i.e., CO, higher order hydrocarbons and oxygenates, exhibit a rising trend as a function of time, because their net production is higher than their net consumption. The most abundant reaction products are CO, H_2O and CH_4, and to a lower extent also CH_2O, C_2H_6, O_2 and CH_3OH. This is in good agreement with reported results from literature for similar CO_2/H_2 discharges. Altering the inlet gas mixing ratio did not drastically affect the densities of the formed higher hydrocarbons and oxygenates, as the conversion of CO_2 was found to be very low in all gas mixing ratios. We have also presented the calculated conversions of the inlet gases and the maximum yields and corresponding selectivities of the main reaction products. It is clear that the conversion of CO_2 is rather low (i.e., in the order of 2-7 %) in all gas mixtures, and much lower than in a CO_2/CH_4 mixture, where typical conversions in the order of 3-20 % are obtained at similar conditions. The reason is the abundance of CH_2 radicals in the latter mixture, which significantly contribute to the loss of CO_2, but their density is very low in the CO_2/H_2 mixture. The H_2 conversion was calculated to be about 30-60 %, depending on the gas mixing ratio. CO was found to be the only value-added end product with a high selectivity.

Note that the gas conversion might be slightly underestimated in the model, because the 1D fluid model does not account for filament formation in the DBD reactor, but simply assumes a

homogeneous plasma. Hence, the calculated mean electron energy in this model might be somewhat lower than typical values expected inside the microdischarge filaments, although the values obtained in our model are still in the same order as typical values reported for the filaments in literature.[4, 114] As a consequence, electron impact excitation, ionization and dissociation reactions might be slightly underestimated, but we expect that the effect will be minor. Moreover, the subsequent plasma chemistry governing the gas conversion is mainly attributed to radical reactions, which also occur in between the filaments, so we expect that the calculations still give a realistic picture of the plasma chemistry. This can also be deduced from the reasonable agreement with experimental data from literature, for the CO_2/H_2 mixture, but also for the pure CH_4 plasma and the CH_4/CO_2 and CH_4/O_2 mixtures that we investigated previously, using the same model assumptions.[87, 108] It needs to be mentioned, however, that an alternative, and probably better, approach to model the plasma chemistry in a DBD reactor is to apply a 0D model, which describes the plasma chemistry only as a function of time, taking into account a large number of power pulses, mimicking the microdischarge filaments in the DBD reactor, which the gas molecules pass when they travel through the reactor. This approach has been applied for instance in other work from our group.[22, 26-27, 78, 91, 109] Nevertheless, in spite of this completely different approach, similar results in terms of plasma chemistry, gas conversion, and product formation are observed, indicating that the present 1D fluid model is also a reasonable approach to model the gas conversion in a DBD plasma.

Finally, the underlying plasma chemistry governing the conversion of CO_2 and H_2 into the various products was analyzed in detail. The dominant reaction pathways for the consumption of CO_2 and H_2 and the production and loss of some interesting end products, i.e., CO, CH_4, CH_2O, and CH_3OH, were discussed. It is clear from our results that a higher conversion of CO_2, as well

as a higher density of CH_3 and CH_2 radicals, would be necessary in order to obtain higher yields of the desired end products. For the conditions under study, only CO is formed at an acceptable level. Thus, it is clear that a CO_2/H_2 mixture is not very suitable for the production of other value added chemicals besides CO, and a CO_2/CH_4 mixture is more appropriate, because of the presence of CH_2 and CH_3 radicals. The use of a catalyst can possibly increase the formation of some desired oxygenates, as is indeed also shown by Eliasson et al.[95] and Zeng et al.[98]

ACKNOWLEDGMENT

This work was carried out using the Turing HPC infrastructure at the CalcUA core facility of the Universiteit Antwerpen, a division of the Flemish Supercomputer Center VSC, funded by the Hercules Foundation, the Flemish Government (department EWI), and the Universiteit Antwerpen. The authors also acknowledge financial support from the IAP/7 (Interuniversity Attraction Pole) program "PSI-Physical Chemistry of Plasma-Surface Interactions" by the Belgian Federal Office for Science Policy (BELSPO) and from the Fund for Scientific Research Flanders (FWO).

REFERENCES

(1) Intergovernmental Panel on Climate Change *Ipcc Special Report on Carbon Dioxide Capture and Storage*; Cambridge University Press, Cambridge, United Kingdom and New York, NY, USA, 2005.

(2) European Seventh Framework Programme *A Vision for Smart CO_2 Transformation in Europe*; 2015.

(3) Damiani, D.; Litynski, J. T.; McIlvried, H. G.; Vikara, D. M.; Srivastava, R. D. The US Department of Energy's R&D Program to Reduce Greenhouse Gas Emissions through Beneficial Uses of Carbon Dioxide. *Greenhouse Gases: Science and Technology* **2012**, *2*, 9-16.

(4) Bogaerts, A.; De Bie, C.; Snoeckx, R.; Kozák, T. Plasma Based CO_2 and CH_4 Conversion: A Modeling Perspective. *Plasma Process. Polym.* **(in press)**.

(5) Eliasson, B.; Kogelschatz, U. Modeling and Applications of Silent Discharge Plasmas. *IEEE Trans. Plasma Sci.* **1991**, *19*, 309-323.

(6) Conrads, H.; Schmidt, M. Plasma Generation and Plasma Sources. *Plasma Sources Sci. Technol.* **2000**, *9*, 441-454.

(7) Gibalov, V. I.; Pietsch, G. J. The Development of Dielectric Barrier Discharges in Gas Gaps and on Surfaces. *J. Phys. D: Appl. Phys.* **2000**, *33*, 2618-2636.

(8) Bogaerts, A.; Neyts, E.; Gijbels, R.; van der Mullen, J. Gas Discharge Plasmas and Their Applications. *Spectrochim. Acta B* **2002**, *57*, 609-658.

(9) Kogelschatz, U. Filamentary, Patterned, and Diffuse Barrier Discharges. *IEEE Trans. Plasma Sci.* **2002**, *30*, 1400-1408.

(10) Kogelschatz, U. Dielectric-Barrier Discharges: Their History, Discharge Physics, and Industrial Applications. *Plasma Chem. Plasma Process.* **2003**, *23*, 1-46.

(11) Tsuji, M.; Tanoue, T.; Nakano, K.; Nishimura, Y. Decomposition of CO_2 into CO and O in a Microwave-Excited Discharge Flow of CO_2/He or CO_2/Ar Mixtures. *Chem. Lett.* **2001**, *30*, 22-23.

(12) Wen, Y. Z.; Jiang, X. Z. Decomposition of CO_2 Using Pulsed Corona Discharges Combined with Catalyst. *Plasma Chem. Plasma Process.* **2001**, *21*, 665-678.

(13) Mikoviny, T.; Kocan, M.; Matejcik, S.; Mason, N. J.; Skalny, J. D. Experimental Study of Negative Corona Discharge in Pure Carbon Dioxide and Its Mixtures with Oxygen. *J. Phys. D: Appl. Phys.* **2004**, *37*, 64-73.

(14) Indarto, A.; Choi, J.-W.; Lee, H.; Song, H. K. Conversion of CO_2 by Gliding Arc Plasma. *Environ. Eng. Sci.* **2006**, *23*, 1033-1043.

(15) Indarto, A.; Yang, D. R.; Choi, J. W.; Lee, H.; Song, H. K. Gliding Arc Plasma Processing of CO_2 Conversion. *J. Hazard. Mater.* **2007**, *146*, 309-315.

(16) Horvath, G.; Skalny, J. D.; Mason, N. J. FTIR Study of Decomposition of Carbon Dioxide in DC Corona Discharges. *J. Phys. D: Appl. Phys.* **2008**, *41*, 225207.

(17) Spencer, L.; Gallimore, A. D.; Nguyen, S. V. T. Dissociation of CO_2 in a Radio-Frequency Plasma Source. *4th International Congress on Cold Atmospheric Pressure Plasmas: Sources and Applications, Proceedings* **2009**, 130-133.

(18) Paulussen, S.; Verheyde, B.; Tu, X.; De Bie, C.; Martens, T.; Petrovic, D.; Bogaerts, A.; Sels, B. Conversion of Carbon Dioxide to Value-Added Chemicals in Atmospheric Pressure Dielectric Barrier Discharges. *Plasma Sources Sci. Technol.* **2010**, *19*, 034015.

(19) Nunnally, T.; Gutsol, K.; Rabinovich, A.; Fridman, A.; Gutsol, A.; Kemoun, A. Dissociation of CO_2 in a Low Current Gliding Arc Plasmatron. *J. Phys. D: Appl. Phys.* **2011**, *44*, 274009.

(20) Spencer, L. F.; Gallimore, A. D. Efficiency of CO_2 Dissociation in a Radio-Frequency Discharge. *Plasma Chem. Plasma Process.* **2011**, *31*, 79-89.

(21) Vesel, A.; Mozetic, M.; Drenik, A.; Balat-Pichelin, M. Dissociation of CO_2 Molecules in Microwave Plasma. *Chem. Phys.* **2011**, *382*, 127-131.
(22) Aerts, R.; Martens, T.; Bogaerts, A. Influence of Vibrational States on CO_2 Splitting by Dielectric Barrier Discharges. *J. Phys. Chem. C* **2012**, *116*, 23257-23273.
(23) Wang, S.; Zhang, Y.; Liu, X.; Wang, X. Enhancement of CO_2 Conversion Rate and Conversion Efficiency by Homogeneous Discharges. *Plasma Chem. Plasma Process.* **2012**, *32*, 979-989.
(24) Yu, Q. Q.; Kong, M.; Liu, T.; Fei, J. H.; Zheng, X. M. Characteristics of the Decomposition of CO_2 in a Dielectric Packed-Bed Plasma Reactor. *Plasma Chem. Plasma Process.* **2012**, *32*, 153-163.
(25) Spencer, L. F.; Gallimore, A. D. CO_2 Dissociation in an Atmospheric Pressure Plasma/Catalyst System: A Study of Efficiency. *Plasma Sources Sci. Technol.* **2013**, *22*, 015019.
(26) Kozak, T.; Bogaerts, A. Splitting of CO_2 by Vibrational Excitation in Non-Equilibrium Plasmas: A Reaction Kinetics Model. *Plasma Sources Sci. Technol.* **2014**, *23*, 045004.
(27) Aerts, R.; Somers, W.; Bogaerts, A. Carbon Dioxide Splitting in a Dielectric Barrier Discharge Plasma: A Combined Experimental and Computational Study. *ChemSusChem* **2015**, *8*, 702-716.
(28) Van Laer, K.; Bogaerts, A. Improving the Conversion and Energy Efficiency of Carbon Dioxide Splitting in a Zirconia-Packed Dielectric Barrier Discharge Reactor. *Energy Technology* **2015**, *3*, 1038-1044.
(29) Yap, D.; Tatibouet, J. M.; Batiot-Dupeyrat, C. Carbon Dioxide Dissociation to Carbon Monoxide by Non-Thermal Plasma. *J. CO2 Util.* **2015**, *12*, 54-61.
(30) Belov, I.; Paulussen, S.; Bogaerts, A. Appearance of a Conductive Carbonaceous Coating in a CO_2 Dielectric Barrier Discharge and Its Influence on the Electrical Properties and the Conversion Efficiency. *Plasma Sources Sci. Technol.* **2016**, *25*, 015023.
(31) Chen, G. X.; Georgieva, V.; Godfroid, T.; Snyders, R.; Delplancke-Ogletree, M. P. Plasma Assisted Catalytic Decomposition of CO_2. *Appl. Catal. B-Environ.* **2016**, *190*, 115-124.
(32) Mei, D. H.; Zhu, X. B.; Wu, C. F.; Ashford, B.; Williams, P. T.; Tu, X. Plasma-Photocatalytic Conversion of CO_2 at Low Temperatures: Understanding the Synergistic Effect of Plasma-Catalysis. *Appl. Catal. B-Environ.* **2016**, *182*, 525-532.
(33) Ozkan, A.; Dufour, T.; Silva, T.; Britun, N.; Snyders, R.; Bogaerts, A.; Reniers, F. The Influence of Power and Frequency on the Filamentary Behavior of a Flowing DBD-Application to the Splitting of CO_2. *Plasma Sources Sci. Technol.* **2016**, *25*, 025013.
(34) Ponduri, S.; Becker, M. M.; Welzel, S.; van de Sanden, M. C. M.; Loffhagen, D.; Engeln, R. Fluid Modelling of CO_2 Dissociation in a Dielectric Barrier Discharge. *J. Appl. Phys.* **2016**, *119*, 093301.
(35) Ray, D.; Subrahmanyam, C. CO_2 Decomposition in a Packed DBD Plasma Reactor: Influence of Packing Materials. *RSC Advances* **2016**, *6*, 39492-39499.
(36) Larkin, D. W.; Caldwell, T. A.; Lobban, L. L.; Mallinson, R. G. Oxygen Pathways and Carbon Dioxide Utilization in Methane Partial Oxidation in Ambient Temperature Electric Discharges. *Energ. Fuel.* **1998**, *12*, 740-744.
(37) Zhou, L. M.; Xue, B.; Kogelschatz, U.; Eliasson, B. Nonequilibrium Plasma Reforming of Greenhouse Gases to Synthesis Gas. *Energ. Fuel.* **1998**, *12*, 1191-1199.
(38) Eliasson, B.; Liu, C. J.; Kogelschatz, U. Direct Conversion of Methane and Carbon Dioxide to Higher Hydrocarbons Using Catalytic Dielectric-Barrier Discharges with Zeolites. *Ind. Eng. Chem. Res.* **2000**, *39*, 1221-1227.
(39) Huang, A. M.; Xia, G. G.; Wang, J. Y.; Suib, S. L.; Hayashi, Y.; Matsumoto, H. CO_2 Reforming of CH_4 by Atmospheric Pressure AC Discharge Plasmas. *J. Catal.* **2000**, *189*, 349-359.
(40) Kozlov, K. V.; Michel, P.; Wagner, H. E. Synthesis of Organic Compounds from Mixtures of Methane with Carbon Dioxide in Dielectric-Barrier Discharges at Atmospheric Pressure. *Plasmas Polym.* **2000**, *5*, 129-150.

(41) Yao, S. L.; Ouyang, F.; Nakayama, A.; Suzuki, E.; Okumoto, N.; Mizuno, A. Oxidative Coupling and Reforming of Methane with Carbon Dioxide Using a High-Frequency Pulsed Plasma. *Energ. Fuel.* **2000**, *14*, 910-914.
(42) Kraus, M.; Eliasson, B.; Kogelschatz, U.; Wokaun, A. CO_2 Reforming of Methane by the Combination of Dielectric-Barrier Discharges and Catalysis. *Phys. Chem. Chem. Phys.* **2001**, *3*, 294-300.
(43) Liu, C. J.; Xue, B. Z.; Eliasson, B.; He, F.; Li, Y.; Xu, G. H. Methane Conversion to Higher Hydrocarbons in the Presence of Carbon Dioxide Using Dielectric-Barrier Discharge Plasmas. *Plasma Chem. Plasma Process.* **2001**, *21*, 301-310.
(44) Yao, S. L.; Okumoto, M.; Nakayama, A.; Suzuki, E. Plasma Reforming and Coupling of Methane with Carbon Dioxide. *Energ. Fuel.* **2001**, *15*, 1295-1299.
(45) Zhang, K.; Kogelschatz, U.; Eliasson, B. Conversion of Greenhouse Gases to Synthesis Gas and Higher Hydrocarbons. *Energ. Fuel.* **2001**, *15*, 395-402.
(46) Jiang, T.; Li, Y.; Liu, C. J.; Xu, G. H.; Eliasson, B.; Xue, B. Z. Plasma Methane Conversion Using Dielectric-Barrier Discharges with Zeolite A. *Catal. Today* **2002**, *72*, 229-235.
(47) Li, Y.; Liu, C. J.; Eliasson, B.; Wang, Y. Synthesis of Oxygenates and Higher Hydrocarbons Directly from Methane and Carbon Dioxide Using Dielectric-Barrier Discharges: Product Distribution. *Energ. Fuel.* **2002**, *16*, 864-870.
(48) Zhang, X. L.; Dai, B.; Zhu, A. M.; Gong, W. M.; Liu, C. H. The Simultaneous Activation of Methane and Carbon Dioxide to C_2 Hydrocarbons under Pulse Corona Plasma over La_2O_3/gamma-Al_2O_3 Catalyst. *Catal. Today* **2002**, *72*, 223-227.
(49) Zhang, K.; Eliasson, B.; Kogelschatz, U. Direct Conversion of Greenhouse Gases to Synthesis Gas and C_4 Hydrocarbons over Zeolite HY Promoted by a Dielectric-Barrier Discharge. *Ind. Eng. Chem. Res.* **2002**, *41*, 1462-1468.
(50) Hwang, B.; Yeo, Y.; Na, B. Conversion of CH_4 and CO_2 to Syngas and Higher Hydrocarbons Using Dielectric Barrier Discharge. *Korean J. Chem. Eng.* **2003**, *20*, 631-634.
(51) Zhang, J. Q.; Zhang, J. S.; Yang, Y. J.; Liu, Q. Oxidative Coupling and Reforming of Methane with Carbon Dioxide Using a Pulsed Microwave Plasma under Atmospheric Pressure. *Energ. Fuel.* **2003**, *17*, 54-59.
(52) Zhang, Y. P.; Li, Y.; Wang, Y.; Liu, C. J.; Eliasson, B. Plasma Methane Conversion in the Presence of Carbon Dioxide Using Dielectric-Barrier Discharges. *Fuel Process. Technol.* **2003**, *83*, 101-109.
(53) Zou, J. J.; Zhang, Y. P.; Liu, C. J.; Li, Y.; Eliasson, B. Starch-Enhanced Synthesis of Oxygenates from Methane and Carbon Dioxide Using Dielectric-Barrier Discharges. *Plasma Chem. Plasma Process.* **2003**, *23*, 69-82.
(54) Song, H. K.; Choi, J. W.; Yue, S. H.; Lee, H.; Na, B. K. Synthesis Gas Production Via Dielectric Barrier Discharge over Ni/gamma-Al_2O_3 Catalyst. *Catal. Today* **2004**, *89*, 27-33.
(55) Song, H. K.; Lee, H.; Choi, J.-W.; Na, B.-k. Effect of Electrical Pulse Forms on the CO_2 Reforming of Methane Using Atmospheric Dielectric Barrier Discharge. *Plasma Chem. Plasma Process.* **2004**, *24*, 57-72.
(56) Indarto, A.; Choi, J.-W.; Lee, H.; Song, H. K. Effect of Additive Gases on Methane Conversion Using Gliding Arc Discharge. *Energy* **2006**, *31*, 2986-2995.
(57) Istadi, I.; Amin, N. A. S. Co-Generation of Synthesis Gas and C_{2+} Hydrocarbons from Methane and Carbon Dioxide in a Hybrid Catalytic-Plasma Reactor: A Review. *Fuel* **2006**, *85*, 577-592.
(58) Li, M. W.; Tian, Y. L.; Xu, G. H. Characteristics of Carbon Dioxide Reforming of Methane Via Alternating Current (AC) Corona Plasma Reactions. *Energ. Fuel.* **2007**, *21*, 2335-2339.
(59) Li, D. H.; Li, X.; Bai, M. G.; Tao, X. M.; Shang, S. Y.; Dai, X. Y.; Yin, Y. X. CO_2 Reforming of CH_4 by Atmospheric Pressure Glow Discharge Plasma: A High Conversion Ability. *Int. J. Hydrogen Energ.* **2009**, *34*, 308-313.

(60) Wang, Q.; Yan, B. H.; Jin, Y.; Cheng, Y. Dry Reforming of Methane in a Dielectric Barrier Discharge Reactor with Ni/Al_2O_3 Catalyst: Interaction of Catalyst and Plasma. *Energ. Fuel.* **2009**, *23*, 4196-4201.
(61) Wang, Q.; Yan, B. H.; Jin, Y.; Cheng, Y. Investigation of Dry Reforming of Methane in a Dielectric Barrier Discharge Reactor. *Plasma Chem. Plasma Process.* **2009**, *29*, 217-228.
(62) Wang, Q.; Cheng, Y.; Jin, Y. Dry Reforming of Methane in an Atmospheric Pressure Plasma Fluidized Bed with Ni/gamma-Al_2O_3 Catalyst. *Catal. Today* **2009**, *148*, 275-282.
(63) Rico, V. J.; Hueso, J. L.; Cotrino, J.; Gonzalez-Elipe, A. R. Evaluation of Different Dielectric Barrier Discharge Plasma Configurations as an Alternative Technology for Green C_1 Chemistry in the Carbon Dioxide Reforming of Methane and the Direct Decomposition of Methanol. *J. Phys. Chem. A* **2010**, *114*, 4009-4016.
(64) Sentek, J.; Krawczyk, K.; Mlotek, M.; Kalczewska, M.; Kroker, T.; Kolb, T.; Schenk, A.; Gericke, K. H.; Schmidt-Szalowski, K. Plasma-Catalytic Methane Conversion with Carbon Dioxide in Dielectric Barrier Discharges. *Appl. Catal. B-Environ.* **2010**, *94*, 19-26.
(65) Seyed-Matin, N.; Jalili, A. H.; Jenab, M. H.; Zekordi, S. M.; Afzali, A.; Rasouli, C.; Zamaniyan, A. DC-Pulsed Plasma for Dry Reforming of Methane to Synthesis Gas. *Plasma Chem. Plasma Process.* **2010**, *30*, 333-347.
(66) Yan, B. H.; Wang, Q.; Jin, Y.; Cheng, Y. Dry Reforming of Methane with Carbon Dioxide Using Pulsed DC Arc Plasma at Atmospheric Pressure. *Plasma Chem. Plasma Process.* **2010**, *30*, 257-266.
(67) Goujard, V.; Tatibouet, J. M.; Batiot-Dupeyrat, C. Carbon Dioxide Reforming of Methane Using a Dielectric Barrier Discharge Reactor: Effect of Helium Dilution and Kinetic Model. *Plasma Chem. Plasma Process.* **2011**, *31*, 315-325.
(68) Machrafi, H.; Cavadias, S.; Amouroux, J. CO_2 Valorization by Means of Dielectric Barrier Discharge. *J. Phys.: Conf. Ser.* **2011**, *275*, 012016.
(69) Pinhão, N. R.; Janeco, A.; Branco, J. B. Influence of Helium on the Conversion of Methane and Carbon Dioxide in a Dielectric Barrier Discharge. *Plasma Chem. Plasma Process.* **2011**, *31*, 427-439.
(70) Scarduelli, G.; Guella, G.; Ascenzi, D.; Tosi, P. Synthesis of Liquid Organic Compounds from CH_4 and CO_2 in a Dielectric Barrier Discharge Operating at Atmospheric Pressure. *Plasma Process. Polym.* **2011**, *8*, 25-31.
(71) Schmidt-Szalowski, K.; Krawczyk, K.; Sentek, J.; Ulejczyk, B.; Gorska, A.; Mlotek, M. Hybrid Plasma-Catalytic Systems for Converting Substances of High Stability, Greenhouse Gases and VOC. *Chem. Eng. Res. Des.* **2011**, *89*, 2643-2651.
(72) Tu, X.; Gallon, H. J.; Twigg, M. V.; Gorry, P. A.; Whitehead, J. C. Dry Reforming of Methane over a Ni/Al_2O_3 Catalyst in a Coaxial Dielectric Barrier Discharge Reactor. *J. Phys. D: Appl. Phys.* **2011**, *44*, 274007.
(73) Wang, Q.; Shi, H. L.; Yan, B. H.; Jin, Y.; Cheng, Y. Steam Enhanced Carbon Dioxide Reforming of Methane in DBD Plasma Reactor. *Int. J. Hydrogen Energ.* **2011**, *36*, 8301-8306.
(74) Gallon, H. J.; Tu, X.; Whitehead, J. C. Effects of Reactor Packing Materials on H_2 Production by CO_2 Reforming of CH_4 in a Dielectric Barrier Discharge. *Plasma Process. Polym.* **2012**, *9*, 90-97.
(75) Kim, T. K.; Lee, W. G. Reaction between Methane and Carbon Dioxide to Produce Syngas in Dielectric Barrier Discharge System. *J. Ind. Eng. Chem.* **2012**, *18*, 1710-1714.
(76) Kolb, T.; Kroker, T.; Voigt, J. H.; Gericke, K. H. Wet Conversion of Methane and Carbon Dioxide in a DBD Reactor. *Plasma Chem. Plasma Process.* **2012**, *32*, 1139-1155.
(77) Tu, X.; Whitehead, J. C. Plasma-Catalytic Dry Reforming of Methane in an Atmospheric Dielectric Barrier Discharge: Understanding the Synergistic Effect at Low Temperature. *Appl. Catal. B-Environ.* **2012**, *125*, 439-448.
(78) Snoeckx, R.; Aerts, R.; Tu, X.; Bogaerts, A. Plasma-Based Dry Reforming: A Computational Study Ranging from the Nanoseconds to Seconds Time Scale. *J. Phys. Chem. C* **2013**, *117*, 4957-4970.

(79) Zhang, X. M.; Cha, M. S. Electron-Induced Dry Reforming of Methane in a Temperature-Controlled Dielectric Barrier Discharge Reactor. *J. Phys. D: Appl. Phys.* **2013**, *46*, 415205.
(80) Chung, W. C.; Pan, K. L.; Lee, H. M.; Chang, M. B. Dry Reforming of Methane with Dielectric Barrier Discharge and Ferroelectric Packed-Bed Reactors. *Energ. Fuel.* **2014**, *28*, 7621-7631.
(81) Krawczyk, K.; Mlotek, M.; Ulejczyk, B.; Schmidt-Szalowski, K. Methane Conversion with Carbon Dioxide in Plasma-Catalytic System. *Fuel* **2014**, *117*, 608-617.
(82) Martini, L. M.; Dilecce, G.; Guella, G.; Maranzana, A.; Tonachini, G.; Tosi, P. Oxidation of CH_4 by CO_2 in a Dielectric Barrier Discharge. *Chem. Phys. Lett.* **2014**, *593*, 55-60.
(83) Pan, K. L.; Chung, W. C.; Chang, M. B. Dry Reforming of CH_4 with CO_2 to Generate Syngas by Combined Plasma Catalysis. *IEEE Trans. Plasma Sci.* **2014**, *42*, 3809-3818.
(84) Scapinello, M.; Martini, L. M.; Tosi, P. CO_2 Hydrogenation by CH_4 in a Dielectric Barrier Discharge: Catalytic Effects of Nickel and Copper. *Plasma Process. Polym.* **2014**, *11*, 624-628.
(85) Tu, X.; Whitehead, J. C. Plasma Dry Reforming of Methane in an Atmospheric Pressure AC Gliding Arc Discharge: Co-Generation of Syngas and Carbon Nanomaterials. *Int. J. Hydrogen Energ.* **2014**, *39*, 9658-9669.
(86) Abd Allah, Z.; Whitehead, J. C. Plasma-Catalytic Dry Reforming of Methane in an Atmospheric Pressure AC Gliding Arc Discharge. *Catal. Today* **2015**, *256*, 76-79.
(87) De Bie, C.; van Dijk, J.; Bogaerts, A. The Dominant Pathways for the Conversion of Methane into Oxygenates and Syngas in an Atmospheric Pressure Dielectric Barrier Discharge. *J. Phys. Chem. C* **2015**, *119*, 22331-22350.
(88) Janeco, A.; Pinhao, N. R.; Guerra, V. Electron Kinetics in $He/CH_4/CO_2$ Mixtures Used for Methane Conversion. *J. Phys. Chem. C* **2015**, *119*, 109-120.
(89) Kameshima, S.; Tamura, K.; Ishibashi, Y.; Nozaki, T. Pulsed Dry Methane Reforming in Plasma-Enhanced Catalytic Reaction. *Catal. Today* **2015**, *256*, 67-75.
(90) Ozkan, A.; Dufour, T.; Arnoult, G.; De Keyzer, P.; Bogaerts, A.; Reniers, F. CO_2-CH_4 Conversion and Syngas Formation at Atmospheric Pressure Using a Multi-Electrode Dielectric Barrier Discharge. *J. CO2 Util.* **2015**, *9*, 74-81.
(91) Snoeckx, R.; Zeng, Y. X.; Tu, X.; Bogaerts, A. Plasma-Based Dry Reforming: Improving the Conversion and Energy Efficiency in a Dielectric Barrier Discharge. *RSC Advances* **2015**, *5*, 29799-29808.
(92) Zeng, Y. X.; Zhu, X. B.; Mei, D. H.; Ashford, B.; Tu, X. Plasma-Catalytic Dry Reforming of Methane over gamma-Al_2O_3 Supported Metal Catalysts. *Catal. Today* **2015**, *256*, 80-87.
(93) Zheng, X. G.; Tan, S. Y.; Dong, L. C.; Li, S. B.; Chen, H. M. Plasma-Assisted Catalytic Dry Reforming of Methane: Highly Catalytic Performance of Nickel Ferrite Nanoparticles Embedded in Silica. *J. Power Sources* **2015**, *274*, 286-294.
(94) Scapinello, M.; Martini, L. M.; Dilecce, G.; Tosi, P. Conversion of CH_4/CO_2 by a Nanosecond Repetitively Pulsed Discharge. *J. Phys. D: Appl. Phys.* **2016**, *49*, 075602.
(95) Eliasson, B.; Kogelschatz, U.; Xue, B. Z.; Zhou, L. M. Hydrogenation of Carbon Dioxide to Methanol with a Discharge-Activated Catalyst. *Ind. Eng. Chem. Res.* **1998**, *37*, 3350-3357.
(96) Hayashi, N.; Yamakawa, T.; Baba, S. Effect of Additive Gases on Synthesis of Organic Compounds from Carbon Dioxide Using Non-Thermal Plasma Produced by Atmospheric Surface Discharges. *Vacuum* **2006**, *80*, 1299-1304.
(97) Kano, M.; Satoh, G.; Iizuka, S. Reforming of Carbon Dioxide to Methane and Methanol by Electric Impulse Low-Pressure Discharge with Hydrogen. *Plasma Chem. Plasma Process.* **2012**, *32*, 177-185.
(98) Zeng, Y.; Tu, X. Plasma-Catalytic CO_2 Hydrogenation at Low Temperatures. *IEEE Trans. Plasma Sci.* **2016**, *44*, 405-411.
(99) Jadhav, S. G.; Vaidya, P. D.; Bhanage, B. M.; Joshi, J. B. Catalytic Carbon Dioxide Hydrogenation to Methanol: A Review of Recent Studies. *Chem. Eng. Res. Des.* **2014**, *92*, 2557-2567.

(100) Olah, G. A.; Prakash, G. K. S.; Goeppert, A. Anthropogenic Chemical Carbon Cycle for a Sustainable Future. *J. Am. Chem. Soc.* **2011**, *133*, 12881-12898.
(101) Liu, C. J.; Xu, G. H.; Wang, T. M. Non-Thermal Plasma Approaches in CO_2 Utilization. *Fuel Process. Technol.* **1999**, *58*, 119-134.
(102) Chiavassa, D. L.; Collins, S. E.; Bonivardi, A. L.; Baltanas, M. A. Methanol Synthesis from CO_2/H_2 Using Ga_2O_3-Pd/silica Catalysts: Kinetic Modeling. *Chem. Eng. J.* **2009**, *150*, 204-212.
(103) Tao, X. M.; Wang, J. M.; Li, Z. W.; Ye, Q. G. Theoretical Study on the Reaction Mechanism of CO_2 Hydrogenation to Methanol. *Comput. Theor. Chem.* **2013**, *1023*, 59-64.
(104) van Dijk, J.; Peerenboom, K.; Jimenez, M.; Mihailova, D.; van der Mullen, J. The Plasma Modelling Toolkit Plasimo. *J. Phys. D: Appl. Phys.* **2009**, *42*, 194012.
(105) http://plasimo.phys.tue.nl
(106) Hagelaar, G. J. M. Modeling of Microdischarges for Display Technology. PhD Thesis, Eindhoven University of Technology, Eindhoven, 2000.
(107) Brok, W. J. M.; van Dijk, J.; Bowden, M. D.; van der Mullen, J. J. A. M.; Kroesen, G. M. W. A Model Study of Propagation of the First Ionization Wave During Breakdown in a Straight Tube Containing Argon. *J. Phys. D: Appl. Phys.* **2003**, *36*, 1967-1979.
(108) De Bie, C.; Verheyde, B.; Martens, T.; van Dijk, J.; Paulussen, S.; Bogaerts, A. Fluid Modeling of the Conversion of Methane into Higher Hydrocarbons in an Atmospheric Pressure Dielectric Barrier Discharge. *Plasma Process. Polym.* **2011**, *8*, 1033-1058.
(109) Bogaerts, A.; Wang, W.; Berthelot, A.; Guerra, V. Modeling Plasma-Based CO_2 Conversion: Crucial Role of the Dissociation Cross Section. *Plasma Sources Sci. Technol.* **2016**, *25*, 055016.
(110) Larkin, D. W.; Zhou, L. M.; Lobban, L. L.; Mallinson, R. G. Product Selectivity Control and Organic Oxygenate Pathways from Partial Oxidation of Methane in a Silent Electric Discharge Reactor. *Ind. Eng. Chem. Res.* **2001**, *40*, 5496-5506.
(111) Larkin, D. W.; Lobban, L. L.; Mallinson, R. G. The Direct Partial Oxidation of Methane to Organic Oxygenates Using a Dielectric Barrier Discharge Reactor as a Catalytic Reactor Analog. *Catal. Today* **2001**, *71*, 199-210.
(112) Larkin, D. W.; Lobban, L. L.; Mallinson, R. G. Production of Organic Oxygenates in the Partial Oxidation of Methane in a Silent Electric Discharge Reactor. *Ind. Eng. Chem. Res.* **2001**, *40*, 1594-1601.
(113) Agiral, A.; Nozaki, T.; Nakase, M.; Yuzawa, S.; Okazaki, K.; Gardeniers, J. G. E. Gas-to-Liquids Process Using Multi-Phase Flow, Non-Thermal Plasma Microreactor. *Chem. Eng. J.* **2011**, *167*, 560-566.
(114) Fridman, A., *Plasma Chemistry*; Cambridge University Press: Cambridge, 2008, p 1022.
(115) Belov, I.; Vanneste, J.; Aghaee, M.; Paulussen, S.; Bogaerts, A. Synthesis of Micro- and Nanomaterials in CO_2 and CO Dielectric Barrier Discharges. *Plasma Process. Polym.* **(in press)**.
(116) Van Laer, K.; Bogaerts, A. Fluid Modelling of a Packed Bed Dielectric Barrier Discharge Plasma Reactor. *Plasma Sources Sci. Technol.* **2016**, *25*, 015002.
(117) Mei, D.; Zhu, X.; He, Y.; Yan, J. D.; Tu, X. Plasma-Assisted Conversion of CO_2 in a Dielectric Barrier Discharge Reactor: Understanding the Effect of Packing Materials. *Plasma Sources Science and Technology* **2015**, *24*, 015011.
(118) Neyts, E. C.; Ostrikov, K.; Sunkara, M. K.; Bogaerts, A. Plasma Catalysis: Synergistic Effects at the Nanoscale. *Chem. Rev.* **2015**, *115*, 13408-13446.

Table of Contents Image